nature medicine

https://doi.org/10.1038/s41591-022-01734-1

Accelerated Article Preview

Multiplexed CRISPR-based microfluidic platform for clinical testing of respiratory viruses and identification of SARS-CoV-2 variants

Received: 22 November 2021

Accepted: 3 February 2022

Accelerated Article Preview
Published online: 07 February 2022

Cite this article as: Welch, N. L. et al. Multiplexed CRISPR-based microfluidic platform for clinical testing of respiratory viruses and identification of SARS-CoV-2 variants. *Nature Medicine* https://doi.org/10.1038/s41591-022-01734-1 (2022).

Nicole L. Welch, Meilin Zhu, Catherine Hua, Juliane Weller, Marzieh Ezzaty Mirhashemi, Tien G. Nguyen, Sreekar Mantena, Matthew R. Bauer, Bennett M. Shaw, Cheri M. Ackerman, Sri Gowtham Thakku, Megan W. Tse, Jared Kehe, Marie-Martine Uwera, Jacqueline S. Eversley, Derek A. Bielwaski, Graham McGrath, Joseph Braidt, Jeremy Johnson, Felecia Cerrato, Gage K. Moreno, Lydia A. Krasilnikova, Brittany A. Petros, Gabrielle L. Gionet, Ewa King, Richard C. Huard, Samantha K. Jalbert, Michael L. Cleary, Nicholas A. Fitzgerald, Stacey B. Gabriel, Glen R. Gallagher, Sandra C. Smole, Lawrence C. Madoff, Catherine M. Brown, Matthew W. Keller, Malania M. Wilson, Marie K. Kirby, John R. Barnes, Daniel J. Park, Katherine J. Siddle, Christian T. Happi, Deborah T. Hung, Michael Springer, Bronwyn L. MacInnis, Jacob E. Lemieux, Eric Rosenberg, John A. Branda, Paul C. Blainey, Pardis C. Sabeti & Cameron Myhrvold

Multiplexed CRISPR-based microfluidic platform for clinical testing of respiratory viruses and identification of SARS-CoV-2 variants

Nicole L. Welch[*1,2] Meilin Zhu[1,3], Catherine Hua[1,4], Juliane Weller[1,5], Marzieh Ezzaty Mirhashemi[1], Tien G. Nguyen[1], Sreekar Mantena[1], Matthew R. Bauer[1,6], Bennett M. Shaw[1,4], Cheri M. Ackerman[1,3], Sri Gowtham Thakku[1,7], Megan W. Tse[1,3], Jared Kehe[1,3], Marie-Martine Uwera[1], Jacqueline S. Eversley[4], Derek A. Bielwaski[4], Graham McGrath[4], Joseph Braidt[4], Jeremy Johnson[1], Felecia Cerrato[1], Gage K. Moreno[1], Lydia A. Krasilnikova[1,8], Brittany A. Petros[1,7,9,10], Gabrielle L. Gionet[1], Ewa King,[10], Richard C. Huard[10], Samantha K. Jalbert[11], Michael L. Cleary[11], Nicholas A. Fitzgerald[1], Stacey B. Gabriel[1], Glen R. Gallagher[12], Sandra C. Smole[12], Lawrence C. Madoff[12], Catherine M. Brown[12], Matthew W. Keller[13], Malania M. Wilson[13], Marie K. Kirby[13], John R. Barnes[13], Daniel J. Park[1], Katherine J. Siddle[1,8], Christian T. Happi[1,14,15], Deborah T. Hung[1,16], Michael Springer[9,11], Bronwyn L. MacInnis[1,17], Jacob E. Lemieux[1,4], Eric Rosenberg[4,18], John A. Branda[§18], Paul C. Blainey[§1,3,19], Pardis C. Sabeti[§*1,9,8,19,20], Cameron Myhrvold[§*21].

[1]Broad Institute of MIT and Harvard, Cambridge, MA, USA. [2]Harvard Program in Virology, Division of Medical Sciences, Harvard Medical School, Boston, MA, USA. [3]Department of Biological Engineering, MIT, Cambridge, MA, USA. [4]Division of Infectious Diseases, Department of Medicine, Massachusetts General Hospital, Boston, MA, USA. [5]Wellcome Sanger Institute, Wellcome Genome Campus, Hinxton, UK. [6]Harvard Program in Biological and Biomedical Sciences, Harvard Medical School, Boston, MA 02115, USA. [7]Division of Health Sciences and Technology, Harvard Medical School and MIT, Cambridge, MA, USA. [8]Department of Organismic and Evolutionary Biology, Harvard University, Cambridge, MA, USA.[9]Harvard/MIT MD-PhD Program, Harvard Medical School, Boston, MA, USA. [10]State Health Laboratories, Rhode Island Department of Health, Providence, RI, USA. [11]Department of Systems Biology, Harvard Medical School, Boston, MA, USA. [12]Massachusetts Department of Public Health, Boston, MA, USA. [13]Influenza Division, National Center for Immunization and Respiratory Diseases (NCIRD), Centers for Disease Control and Prevention (CDC), Atlanta, GA, USA.[14]African Centre of Excellence for Genomics of Infectious Diseases (ACEGID), Redeemer"s University, Ede, Osun State, Nigeria. [15]Department of Biological Sciences, College of Natural Sciences, Redeemer"s University, Ede, Osun State, Nigeria. [16]Molecular Biology Department and Center for Computational and Integrative Biology, Massachusetts General Hospital, Boston, MA, USA. [17]Department of Immunology and Infectious Disease, Harvard T.H. Chan School of Public Health, Harvard University, Boston, MA, USA. [18]Department of Pathology, Massachusetts General Hospital and Harvard Medical School, Boston, MA, USA. [19]Koch Institute for Integrative Cancer Research at MIT, Cambridge, MA, USA. [20]Howard Hughes Medical Institute, Chevy Chase, MD, USA. [21]Department of Molecular Biology, Princeton University, Princeton, NJ, USA.

[§] These authors supervised this work.

[*] Address correspondence to; nicole_welch@g.harvard.edu, pardis@broadinstitute.org or cmyhrvol@princeton.edu

Key words: diagnostic, SARS-CoV-2, COVID-19, CRISPR, respiratory viruses, variants, Omicron, multiplexed, high-throughput, quantification

Abstract

The COVID-19 pandemic has demonstrated a clear need for high-throughput, multiplexed, and sensitive assays for detecting SARS-CoV-2 and other respiratory viruses as well as their emerging variants. Here, we present a cost-effective virus and variant detection platform, called microfluidic CARMEN (mCARMEN), that combines CRISPR-based diagnostics and microfluidics with a streamlined workflow for clinical use. We developed the mCARMEN respiratory virus panel (RVP) to test for up to 21 viruses, including SARS-CoV-2, other coronaviruses and both influenza strains, and demonstrated its diagnostic-grade performance on 525 patient specimens in an academic setting and 166 specimens in a clinical setting. We further developed an mCARMEN panel to enable identification of 6 SARS-CoV-2 variant lineages, including Delta and Omicron, and evaluated it on 2,088 patient specimens, with near-perfect concordance to sequencing-based variant classification. Lastly, we implemented a combined Cas13 and Cas12 approach that enables quantitative measurement of SARS-CoV-2 and influenza A viral copies in samples. The mCARMEN platform enables high-throughput surveillance of multiple viruses and variants simultaneously, enabling rapid detection of SARS-CoV-2 variants.

Introduction

COVID-19 has exposed critical gaps in our global infectious disease diagnostic and surveillance capacity[1]. The pandemic rapidly necessitated high-throughput diagnostics to test large populations[2], yet early diagnostic efforts met technical challenges that cost the United States precious time in its early response[3]. Other challenges developed as the pandemic progressed that point towards an additional need for highly multiplexed surveillance technologies. These challenges include the co-circulating human respiratory viruses that cause symptoms similar to COVID-19[4,5] and emerging SARS-CoV-2 variants of concern (VOCs) with mutations that impact viral fitness and clinical disease prognosis[6,7].

An ideal diagnostic would have surveillance capabilities to process hundreds of patient samples simultaneously, detect multiple viruses, differentiate between viral variants, and quantify viral load[8,9]; yet no such test currently exists. As it stands, there is a trade-off between clinically approved high-throughput diagnostics and multiplexed methods in the number of patient samples and/or pathogens tested simultaneously[10–12]. As examples, reverse transcription-quantitative PCR (RT-qPCR) is high-throughput by testing at least 88 samples, but for 1-3 analytes at a time; multiplexed techniques such as Cepheid Xpert Xpress can detect 4 respiratory viruses in up to 16 samples per run, and BioFire can detect 22 respiratory pathogens in 1 sample simultaneously[13]. Only a few clinical diagnostic methods comprehensively detect SARS-CoV-2 variant mutations[14–16] which is why this has largely been achieved through next-generation sequencing (NGS)[17,18], even though it is time-consuming, expensive, and requires bioinformatic expertise to interpret[6,19–22].

CRISPR-based diagnostics offer an alternative approach to detecting multiple viruses and variants[23–25]. CRISPR effector proteins Cas12[26,27] or Cas13[28,29] activate upon CRISPR RNA (crRNA)-target binding which unleashes their collateral cleavage activity on a fluorescent reporter for readout of viral positivity status[30–34]. The crRNA-target binding events are highly specific and altered by the presence of sequence variation. Maximally active crRNA design has been accelerated by machine learning and other computational methods[35]. Nonetheless, most

CRISPR diagnostics detect one to three targets per sample[30,36–39], which is not sufficient for differential diagnosis via comprehensive microbe or variant identification.

To scale up the capabilities of CRISPR-based diagnostics, we developed Combinatorial Arrayed Reactions for Multiplexed Evaluation of Nucleic acids (CARMEN)[40] which parallelizes nucleic acid detection. The first generation of CARMEN, referred to here as CARMEN v1, could detect 169 human-associated viruses in 8 samples simultaneously. In CARMEN v1, samples and Cas13-crRNA complexes remain separately confined for barcoding and emulsification prior to pairwise droplet combination for detection by fluorescence microscopy. This allows each sample to be tested against every crRNA. CARMEN v1 is a powerful proof-of-concept for multiplexed CRISPR-based detection, but it is difficult to use in a clinical setting given its use of custom-made imaging chips and readout hardware, manually intensive 8-10 hour workflow, and low-throughput sample evaluation.

To fulfill the public health need for a clinically relevant surveillance technology that detects multiple viruses and variants quickly, we developed microfluidic CARMEN (mCARMEN). mCARMEN builds on CARMEN v1 and uses commercially available Fluidigm microfluidics and instrumentation. To our knowledge, mCARMEN is the only diagnostic that combines surveillance capabilities into a single technology platform with the ability to test hundreds of samples in a day for multiple respiratory viruses and variants, while also being able to quantify viral genomic copies.

Results

CARMEN implementation on Fluidigm for respiratory virus detection

CARMEN v1[40] is limited by custom instrumentation requirements and labor-intensive protocols which is why we sought to develop a scalable technology that could be broadly implemented. Microfluidic CARMEN (mCARMEN) meets these requirements and eliminates the color-coding and dropletization needs of CARMEN v1 by using commercially available integrated fluidic circuits (IFCs) on the Fluidigm Biomark for <$13 USD per sample (Fluidigm, San Francisco, CA) (Fig. 1a, Supplementary Table 1&2). By leveraging Fluidigm microfluidics, we overcame the need for a custom microscope and chips as well as data analysis expertise, which were required for CARMEN v1. The Fluidigm IFCs use a specific number of assay combinations: 192 samples by 24 detection assays or 96 samples by 96 detection assays which are all spatially separated (Supplementary Table 3). After manual IFC loading, the Fluidigm controller moves the samples and detection assays through individual channels on the IFC until they reach the chip reaction chamber, where they are thoroughly mixed. We measure fluorescence on the Fluidigm Biomark with our custom automated protocols that take images of the IFC chip every 5 minutes for 1-3 hours at 37°C (Extended Data Fig. 1a).

In our first implementation of the mCARMEN platform, we designed a panel to detect 21 clinically relevant human respiratory viruses (Supplementary Table 4). This includes all viruses covered by BioFire RP2.1 - SARS-CoV-2, four other human-associated coronaviruses and both influenza strains - as well as a few additional illness inducing viruses[41]. To generate maximally active virus-specific crRNAs and PCR primers to detect the 21 viruses, we applied the assay design method ADAPT (Activity-informed Design with All-inclusive Patrolling of Targets; described in methods)[35]. We were able to encompass the full genomic diversity of these viral families by including multiple primers, if needed.

We compared the performance of mCARMEN to CARMEN v1 for detecting synthetic DNA fragments recapitulating the 21 viral targets, and found mCARMEN had the same (13 viruses) or better (8 viruses) analytical sensitivity compared with CARMEN v1 (Fig. 1b and 1c, Extended Data Fig. 1b). Both mCARMEN and CARMEN v1 had 100% analytical specificity, but mCARMEN was 100% sensitive to 10^2 copies/µL and 98.4% sensitive to 10^1 copies/µL while CARMEN v1 was only 86% and 77.8% sensitive, respectively. Moreover, the mCARMEN reaction rate is accelerated compared with CARMEN v1, resulting in faster initial detection and signal saturation of targets (Fig. 1d, Extended Data Fig. 1c). This is likely due to the higher temperature at reaction initiation for mCARMEN (37°C) than for CARMEN v1 (25°C), and the extensive sample-detection assay mixing that occurs in the mCARMEN IFC, rather than merged droplets mixing by diffusion in CARMEN v1.

We then benchmarked the performance of both CARMEN diagnostics against RT-qPCR (CDC 2019-nCoV Kit) and/or unbiased metagenomic NGS on patient specimens. We obtained a set of 6 SARS-CoV-2-positive, 4 SARS-CoV-2-negative, and 8 influenza A virus (FLUAV)-positive patient specimens for initial testing. mCARMEN and CARMEN v1 had 100% concordance with RT-qPCR, NGS, and each other (Fig. 1e). We also compared performance using two different fluorescent reporters, RNase Alert (IDT, Coralville, IA) and a custom 6-Uracil-FAM (polyU) reporter[31]. We found enhanced sensitivity when using a polyU fluorescent reporter due to LwaCas13a"s preference to cleave at uracils[28,29] (Supplementary Fig. 1a&b).

Aside from SARS-CoV-2 and influenza viruses, the remaining 19 viruses detectable by mCARMEN lack a recognized gold-standard clinical diagnostic. Thus, we compared mCARMEN to unbiased metagenomic NGS results for the characterization of 58 pre-pandemic unknown samples collected from patients with a presumed upper respiratory infection (Fig. 1f, Supplementary Table 5, Supplementary Fig. 1c&d). Both mCARMEN and NGS detected the same respiratory viruses in 13 specimens (7 FLUAV, 2 HCoV-229E, 1 HCoV-NL63, 1 HCoV-OC43, 1 HMPV, and 1 HRV), neither detected respiratory viruses in 42 specimens, and they had differing results for 3 specimens, with 93% overall concordance based on an average of ~3 million reads per specimen. Nine of the 13 specimens positive by both methods assembled complete genomes while the remaining 3 assembled partial or no genomes but had >10 reads (2 FLUAV, 1 HMPV, 1 HRV). mCARMEN missed 1 virus-positive specimen detected by NGS, a partial FLUAV genome. We found no sequencing reads spanning the mCARMEN amplicon, suggesting degradation was responsible for the result. mCARMEN detected virus in 2 specimens (1 FLUAV, 1 HRV) where NGS did not detect any viral reads. While we cannot rule out false positive results, metagenomic sequencing has been shown to have poor sensitivity for low viral copy samples[5,19,42].

Streamlining mCARMEN for future clinical use

With a drive towards clinical applications, we aimed to optimize the mCARMEN workflow. To do so, we decreased the manual labor and processing time from >8 hours to <5 hours by implementing automated RNA extraction, using a single-step RNA-to-DNA amplification with 1 primer pool, and reducing the duration of detection readout (Fig. 2a, Extended Data Fig. 2a). We then preliminarily evaluated the optimized workflow on 21 SARS-CoV-2 positive and 8 negative patient specimens, and found greater sensitivity over the original two-step amplification method (Extended Data Fig. 2b).

For an end-to-end mCARMEN workflow, we developed software to be used alongside clinical testing to provide patient diagnoses (Supplementary Fig. 2). The software uses the final image

at 1 hour post-reaction initiation as input, then automatically validates controls to make 1 of 3 calls: “detected,” “not detected,” or “invalid” for each combination of sample and crRNA.

Lastly, we wanted to condense mCARMEN for focused clinical use and did so by developing a respiratory virus panel (RVP) to detect 9 of the most clinically-relevant viruses (SARS-CoV-2, HCoV-HKU1, HCoV-OC43, HCoV-NL63, FLUAV, FLUBV, HPIV-3, HRSV, and HMPV) and a human internal control, (RNase P). These nine viruses were included on RVP based on if they heavily circulate in the population and have capacity to cause respiratory virus symptoms, while others were excluded if genomic diversity was difficult to account for concisely, such as HRV[43]. We first conducted range-determining limit of detection (LOD) studies for the 9 viruses on mCARMEN RVP in a research laboratory. The preliminary LOD was within the range of 100-1,000 copies/mL for SARS-CoV-2, FLUAV, FLUBV, HCoV-HKU1, HCoV-NL63, HCoV-OC42, and 1,000-20,000 copies/mL for HPIV-3, HMPV, HRSV (Extended Data Fig. 3a, Supplementary Table 6), with robust performance from the SARS-CoV-2 crRNA as well as all RVP crRNAs in combination (median AUCs of 1 and 0.989, respectively) (Extended Data Fig. 3b-g).

To benchmark mCARMEN RVP performance to comparator assay results, we analyzed 385 SARS-CoV-2-positive and 140 negative patient specimens, and compared these results to both prior and concurrent RT-qPCR evaluation (Fig. 2b). By the time of comparative evaluation the number of RT-qPCR positive specimens dropped from 385 to 316, suggesting significant viral degradation either from extended sample storage or multiple freeze-thaw cycles. Nonetheless, mCARMEN was able to identify all 316 (100% sensitivity) of the concurrent RT-qPCR positive specimens. We noted mCARMEN further detected SARS-CoV-2 in 42 specimens that tested positive by prior RT-qPCR, but were missed by concurrent RT-qPCR testing suggesting mCARMEN is more robust to low viral quantity.

To confirm RT-qPCR sensitivity relative to mCARMEN, we tested the impact of multiple freeze thaw cycles at several concentrations of SARS-CoV-2 seed stock on assay reproducibility. We found the freeze thaw cycles had no impact on mCARMEN sensitivity across all concentrations, while RT-qPCR was negatively impacted by freeze thaw cycles at the lowest concentration implying the 42 discrepant specimens had low initial viral quantities (Supplementary Fig. 3a-d).

Indeed, if we categorize putative true positives as all specimens that tested positive by prior RT-qPCR as well as present-day RT-qPCR and/or mCARMEN, mCARMEN would have 100% sensitivity compared to 88% for RT-qPCR. mCARMEN also detected SARS-CoV-2 in 3 specimens that tested negative by both prior and concurrent RT-qPCR (Supplementary Fig. 3d). While we cannot rule out the possibility of false-positives, several pieces of evidence suggest they are more likely to be true positives: mCARMEN demonstrates higher sensitivity over concurrent RT-qPCR testing, these specimens are from suspected SARS-CoV-2 cases based on clinical features, and mCARMEN did not detect SARS-CoV-2 in any clinical specimens prior to the pandemic (Fig. 1, Supplementary Fig. 1).

We further evaluated the analytical sensitivity of RVP by correlating RVP fluorescence signals to Ct values obtained from concurrent RT-qPCR testing (CDC 2019-nCoV). Of the 316 specimens positive for SARS-CoV-2 by mCARMEN RVP and both RT-qPCR results, 217 had Ct values <30, suggesting moderate-to-high viral genome copies. By RVP, all 217 specimens (100%) reached signal saturation by 1 hour post-reaction initiation (Fig. 2c&d, Supplementary Fig. 3e). The remaining 100 specimens had Ct values between 30-36 and all but 6 samples (94%) reached signal saturation by 1 hour. In total, 98% (311/316) of the specimens reached saturation by 1 hour indicating mCARMEN can rapidly deem viral positivity status for a range of Ct values. Even 17 of the 42 (~40%) RVP positive specimens, but not concurrently RT-qPCR

positive, reached saturation by 1 hour; the slower saturation of the remaining 25 specimens further suggests detection issues caused by low viral genome copy number (Extended Data Fig. 4a-c). We also evaluated RVP fluorescence for detecting an internal control and human housekeeping gene, RNase P. We found 520 of the 525 (99%) patient specimens reached saturation for RNase P by 1 hour (Extended Data Fig. 4d, described in methods).

Additionally, we used unbiased metagenomic NGS as a metric to evaluate RVP performance. As controls for NGS, we sequenced a set of true SARS-CoV-2 negative specimens (i.e., negative by all three results, RVP and 2x RT-qPCR) (n=16), and true SARS-CoV-2 positives (n=15) with a range of Ct values (15-34) (Extended Data Fig. 4e, Supplementary Table 5). Fifteen out of the 16 true negatives had no more than 2 reads mapped to the SARS-CoV-2 genome, in line with <10 reads expected for negative specimens, while 1 specimen had 11 reads by NGS (average ~8.8 million reads per specimen). All true positive specimens had >10 aligned viral reads, ranging from 16 to 802,306 reads, by NGS (100% sensitivity). Only specimens with Ct values <25 (n=8) were able to assemble complete genomes, while specimens with Ct values >25 (n=7) had <200 reads map to SARS-CoV-2.

By NGS, we then evaluated 22 RVP and RT-qPCR discordant specimens, and 8 specimens for which RVP detected other respiratory viruses. The 22 discordant samples included 13 positive by RVP and prior testing but concurrently negative by RT-qPCR, 6 positive by prior testing, but negative by concurrent RVP and RT-qPCR, and 3 positive by RVP but negative by both RT-qPCR results. All but 1 of the 22 (95%) discordant specimens had <10 viral reads by NGS. The single specimen with >10 reads was positive by RVP and prior RT-qPCR, but not concurrent testing, yet just 22 reads mapped to SARS-CoV-2. NGS additionally failed to detect other respiratory viruses in the 8 RVP-positive specimens. RVP identified 4 SARS-CoV-2 co-infections (2 HCoV-HKU1, 1 HPIV-3 and 1 HRSV), and 4 viruses in SARS-CoV-2-negative specimens (3 FLUAV and 1 HCoV-NL63). Given these specimens also had <10 viral reads aligned by NGS, we can neither validate our results as positive nor rule out the possibility of false-negatives by NGS; these samples are likely low viral quantity implying mCARMEN and RT-qPCR are more sensitive.

Evaluation of RVP performance in a clinical setting

We implemented mCARMEN RVP in the CLIA-certified Clinical Microbiology Laboratory at Massachusetts General Hospital (MGH) to establish assay sensitivity and specificity for clinical validation following FDA guidelines. We first evaluated the limit of detection (LOD), defined as the lowest concentration yielding positive results for at least 19 of 20 replicates. After recapitulating the 9 viral targets on RVP, we found the LOD for HCoV-HKU1, HCoV-NL63, HCoV-OC43, FLUAV, and FLUBV were 500 copies/mL while HMPV and SARS-CoV-2 were 1,000 copies/mL, and HPIV-3 and HRSV were 10,000 copies/mL (Fig. 3a&b, Extended Data Fig. 5a, Supplementary Table 7). The LOD likely varies between viral targets for a few reasons: the crRNAs have varying activity levels on their intended target and differing input materials were used based on sample availability.

After establishing the single analyte LODs, we asked whether co-infections impacted the sensitivity for each virus detected by RVP. To do so, we added SARS-CoV-2 at a constant, 2x LOD, concentration to the remaining 8 viruses on RVP at varying concentrations at or above their respective LOD (Extended Data Fig. 5b). We observed no loss in our ability to detect SARS-CoV-2. However, we noticed a decrease in signal intensity for the other viruses at lower concentrations, yet only one virus, HPIV-3, had a 10-fold higher LOD.

Although we observed no cross-reactivity between RVP panel members in the research setting (Fig. 1 and 2), we followed FDA guidelines to conduct more stringent assay inclusivity and specificity analyses against common respiratory flora and other viral pathogens. *In silico* analysis revealed the primers on RVP are >92% inclusive of the known genetic diversity of each viral species, with additional inclusivity coming from crRNA-target recognition, for an overall >95% inclusivity (Supplementary Table 8). When examining off-target activity *in silico*, FDA defines cross-reactivity as >80% homology between one of the primers or probes to any microorganism. We found no more than 75% homology between the RVP primer and crRNA sequences to other closely related human pathogens (Supplementary Table 9). This implies that off-target detection will rarely, if ever, occur.

Following *in silico* analysis, we evaluated RVP specificity experimentally. We computationally designed position-matched synthetic gene fragments from closely related viral species, including both human- and non-human-infecting species. When evaluating these gene fragments, only SARS-CoV-2 and RaTG13 showed cross-reactivity (Fig. 3c, Extended Data Fig. 6). This cross-reactivity is expected, however, because the RaTG13 amplicon evaluated shares 100% nucleotide identity with the SARS-CoV-2 amplicon in our assay. We did not observe any cross-reactivity when using viral seed stocks, genomic RNA, or synthetic RNA from ATCC or BEI (Supplementary Table 10). Therefore, we found RVP to have 100% analytical specificity.

Finally, the FDA recommends testing a minimum of 30 known-positive clinical specimens for each pathogen in an assay, as well as 30 negative specimens. Where positive specimens are not available, the FDA allows the creation of contrived samples, by spiking viral genomic material at clinically-relevant concentrations into a negative specimen. Each virus evaluated must have a minimum of 95% agreement performance, both positive percent agreement (PPA) and negative (NPA), to clinically-approved comparator assays.

At MGH, archived clinical specimens had been evaluated at the time of collection using one of two comparator assays: Cepheid Xpert Xpress SARS-CoV-2/Flu/RSV multiplexed assay or BioFire RP2.0 multiplexed assay (Extended Data Fig. 7, Supplementary Table 5). These included 166 specimens with 137 total viral clinical results: 31 FLUAV, 30 SARS-CoV-2, 30 HRSV, 29 FLUBV, 8 HMPV, 5 HCoV-NL63, 1 FLUBV and HCoV-NL63 co-infection, 1 HCoV-HKU1,1 HCoV-OC43 and 30 clinically negative. Given these specimens can be degraded by multiple freeze thaws, we concurrently tested all specimens by BioFire RP2.0 or TaqPath COVID-19 Combo Kit for the SARS-CoV-2 specimens. We also supplemented this evaluation with 30 contrived samples for each of the following viruses for which we did not have enough positive specimens: HCoV-HKU1, HCoV-OC43, HCoV-NL63, HPIV-3, and HMPV (described in methods), for a total of 150 contrived samples.

All of the RVP viral targets individually had 100% NPA, and all, except HMPV, had >95% PPA to their respective previous comparator assay result, exceeding the minimum clinical performance set by the FDA (Fig. 3d). Of the 137 previously positive clinical results, mCARMEN correctly detected viral nucleic acids 95% (130/137) of the time. For specimens that were evaluated concurrently, mCARMEN and the comparator assay had 9 discordant results (128/137) with equivalent sensitivity for all but the HMPV specimens; BioFire did not detect virus in 3 specimens (1 FLUAV, 1 FLUBV, and 1 HRSV) and mCARMEN did not detect virus in 6 specimens (1 FLUAV, 1 FLUBV, 1 HRSV, and 3 HMPV). Both mCARMEN and BioFire identified 5 specimens with co-infections (HCoV-NL63 in a FLUAV specimen, HPIV-3 in a FLUBV specimen, HCoV-HKU-1 in 2 HRSV specimens, and HCoV-NL63 in a HRSV specimen). Together with the original clinically detected co-infection, there were 6 (1.1%) co-infections in our specimen set (Extended Data Fig. 5c). Overall, mCARMEN and BioFire were 99.4%

(1485/1494 individual tests) concordant (Fig. 3e, Extended Data Fig. 7). For the contrived samples, mCARMEN correctly identified 99% (148/150) (Fig. 3e).

We used unbiased metagenomic NGS to further evaluate 9 discordant specimens (2 FLUAV, 2 FLUBV, 2 HRSV, and 3 HMPV), generating an average of 13 million reads per specimen. Either no viral reads were present by NGS or partial genomes were assembled, but the RVP amplicon was missing, making it unlikely for our assay to return a positive result (Extended Data Fig. 7, Supplementary Table 5). Based on these results and our previous NGS testing, which indicated NGS was not as sensitive as RVP or the comparator assays, we cannot determine the viral positivity status of these specimens.

Quantification of viral copies using Cas12 and Cas13 kinetics

Similar to widely-used multiplexed approaches, like BioFire[13], the original design of CARMEN[40] did not provide a true quantitative assessment of viral genome copies present in a sample. Establishing the total viral quantity in a patient is important for assessing the stage of infection, transmission risk, and most effective treatment plan[8,9]. The gold standard assay for sample quantification, RT-qPCR, leverages the standard curve - serial dilutions of a given target at a known concentration - as a means of using Ct values to approximate viral quantity[44]. We wanted to determine if a similar approach could be applied to mCARMEN.

To make mCARMEN quantitative, we took advantage of the existence of multiple CRISPR/Cas proteins with differing reaction kinetics and enzymatic activities, and the 3 fluorescent channels detected by the Fluidigm Biomark (Fig. 4a). We incorporated DNA-targeting CRISPR/Cas12 into the Cas13 reaction, and used protein-specific reporters in different fluorescent channels, HEX and FAM, respectively to maximize our multiplexing capabilities. To capture reaction kinetics, images of the IFC chip are taken every 5 minutes for 3 hours to generate sigmoidal curves from the fluorescent signals over time. When considering enzymatic activities, Cas13 has enhanced sensitivity compared to Cas12 since the process of reverse transcribing the dsDNA sample input for Cas13 detection results in increased starting concentration. Thus, we use Cas12 to capture the kinetic curves of higher copy material on the standard curve and Cas13 to capture lower copy material.

We integrated our quantification efforts into RVP, since this assay was extensively evaluated in both research and clinical settings. We manually designed Cas12 crRNAs in the same region of the viral genome that the RVP Cas13 crRNAs target for a two-step standard curve generation on the same target amplicon for Cas12- and Cas13-RNPs individually. The first step requires plotting the fluorescence for a range of concentrations (Cas12: 10^7-10^3 copies/µL; Cas13: 10^3-10^0 copies/µL) at each time point to calculate the IC_{50} through a sigmoidal, four parameter logistic (4PL) curve, R^2 >0.9 (Fig. 4b, Extended Data Fig. 8). In some cases, we could not determine the IC_{50} value because signal saturation occurred too quickly or not at all and therefore, that concentration was excluded from analysis. In the second step, we plotted the IC_{50} values onto a semilog line, where concentration is logarithmic and time is linear, to generate the standard curves (Fig. 4c). We compared these results to a standard curve generated from RT-qPCR using the same serial dilutions and found a linear relationship between SARS-CoV-2 and FLUAV IC_{50} values to Ct values (R^2 0.901 and 0.881, respectively) (Fig. 4d). In all, these results suggest that by using Cas12 and Cas13 in combination, we could extrapolate viral quantification - spanning a 10^0-10^6 range of target concentrations - from patient specimens with performance similar to RT-qPCR.

Allelic discrimination distinguishes between SARS-CoV-2 variant lineages

Since current clinical diagnostics are not well positioned to identify mutations - single nucleotide polymorphisms (SNPs), insertions, or deletions - carried in SARS-CoV-2 variant lineages[6,17,18], we wanted to develop a single platform with both diagnostic and surveillance capabilities for comprehensive detection of 26 SARS-CoV-2 spike gene mutations. We selected these 26 mutations to distinguish between or to detect mutations shared amongst the Alpha, Beta, Gamma, Delta, and Epsilon variant lineages (Supplementary Table 11; B.1.1.7, B.1.351, P.1, B.1.617.2, and B.1.427/9 using PANGO nomenclature system, respectively; WHO Tracking SARS-CoV-2 variants), and then used a generative sequence design algorithm (manuscript in prep.) to produce crRNAs for allelic discrimination.

With the continuous emergence of mutations that can lead to increased transmissibility or enhanced virulence, we also wanted to greatly streamline assay generation for each new SARS-CoV-2 mutation or variant. Thus, we developed an easily adaptable method to track these changes that we call the mCARMEN variant identification panel (VIP). VIP has two non-overlapping primer pair sets within conserved regions of the spike gene to amplify the full-length sequence for use with any crRNA pair. These 26 crRNA pairs, individually or in combination, allow us to track existing variants as well as identify emerging variants (Fig. 5a). Initially, we tested over 60 combinations of crRNAs on unamplified synthetic material to identify the crRNA pairs with the largest fluorescence ratio for expected divided by unexpected signal at each mutation (Supplementary Fig. 4).

We validated the flexible VIP method by testing RNA extracted from SARS-CoV-2 viral seed stocks, for the ancestral (Washington isolate: USA-WA1, ATCC) lineage, and Alpha, Beta, Gamma, Delta, and Epsilon lineages (Fig. 5b, Extended Data Fig. 9). As expected, the WA SARS-CoV-2 viral seed stock isolate showed ancestral signals for all mutations tested. Alpha, Beta, Gamma, Delta, and Epsilon had expected signals for every mutation confirmed by NGS (Supplementary Table 11, description in methods). Though each crRNA has different kinetics owing to varying hit-calling thresholds, we almost always observed a higher expected signal above the unexpected signal, which is important in the prevention of false positive results (Supplementary Fig. 5).

For clinical relevance, we developed an automated variant calling procedure that evaluates the mutation-specific signal in SARS-CoV-2-positive patient specimens and returns a variant lineage result (Supplementary Fig. 6a, described in methods). For some mutations at the same or similar genomic position we observed cross-reactive signals which we overcame by comparing the maximum fluorescent ratios between those mutations and assigning the positive call to the higher of the two (Supplementary Fig. 6b).

We applied VIP and the analysis pipeline to identify the variant lineage in 101 known SARS-CoV-2-positive patient specimens: 24 Alpha, 23 Beta, 24 Gamma, 6 Delta, and 24 Epsilon. Of the 101 specimens with NGS results, all but 3 (97%) specimens (1 Beta and 2 Gammas) were given the correct variant lineage identification (Fig. 5c&d, Supplementary Fig. 7a, Supplementary Table 5). The Beta specimen had signal for a Beta-specific SNP, K417N, but also had signal for Δ156/57, a Delta-specific SNP. The Gamma specimens had no unique signals and shared signals for mutations overlapping with the Beta lineage resulting in a “Variant not Identified” call.

Focusing on the results for the individual mutations themselves, we found that only 1 mutation, E484K, had more than 5 specimens differ in their results between NGS and VIP (Fig. 5e). The 7 E484K discrepancies are attributed to our comparison of cross-reactive signals between E484K

and T478K, thus new crRNA designs are likely needed to optimally differentiate these signals (Supplementary Fig. 6b, 7b&c). Altogether, we found VIP had 97.7% concordance to NGS at allelic discrimination.

VIP identifies Omicron at local and state-wide levels

In November 2021, the SARS-CoV-2 variant lineage, Omicron (BA.1), was first identified by NGS in South Africa and was quickly associated with a rapid increase in case counts (WHO Coronavirus (COVID-19) Dashboard)[45,46]. By December, Omicron was detected in the US and has since driven the recent global COVID-19 wave[47]. However, detection and tracking of Omicron has been challenging, with NGS reporting lagging behind by 7-14 days from collection date. Though S gene target failure (SGTF) by the Thermo Fisher TaqPath COVID-19 Combo Kit can be associated with Omicron, the failure is not specific to Omicron[47,48]. The swift emergence of Omicron has revealed a need for a nucleic-acid based diagnostic with turn-around times similar to RT-PCR, but with mutation-specific information that only NGS currently provides. mCARMEN is uniquely poised to fulfill this need by providing results the same day and ~1 week before NGS.

At the time of Omicron emergence, mCARMEN VIP was already able to uniquely differentiate it from the other SARS-CoV-2 variants by specifically detecting 9 Omicron-tagging mutations amongst our variant panel (Fig. 6a). The unique combination of these spike gene mutations allows for the specificity required to make the proper variant lineage call. In particular, just the combination of S477N and N501Y covers 98.6% of Omicron sequences in GISAID and is 99.997% specific to Omicron (Extended Data Fig. 10a). We rapidly applied VIP to 430 specimens collected at Harvard University CLIA Laboratory (HUCL) from December 6-16 and found the rate of Omicron increased from 15% to 80% in 10 days, overtaking the previously predominant variant, Delta (Fig. 6b, Extended Data Fig. 10b).

Based on the public health importance of this data, the Massachusetts Department of Public Health (MADPH) requested our support for Omicron surveillance across the state. By mCARMEN VIP, we tested 1,557 specimens collected across the state of Massachusetts for the presence of Delta or Omicron from December 13-22 2021. We observed the rate of Omicron increase from ~8% to 77% across Massachusetts in 10 days (Fig. 6c, Extended Data Fig. 10c). In partnership with MADPH and the Broad Genomics Platform, we were able to confirm the mCARMEN variant lineage results with lineage results determined by NGS and found 99.5% (1,549/1,557) concordance between mCARMEN and NGS (Fig. 6d, Extended Data Fig. 10d). Of the 8 discordant samples, 7 had low signal for all mutations evaluated by VIP, suggesting low viral quantity. The remaining discordant specimen had clear signal for several Omicron-specific mutations yet by NGS had Delta signatures, which would suggest likely contamination or sample swap in one of the two tests. In all, mCARMEN VIP was applied in real-time to a local Omicron outbreak and a state-wide Omicron wave with near perfect concordance to NGS, by providing results the same or following day while NGS lagged behind by ~4-7 days (Fig. 6e).

Discussion

Here, we report mCARMEN, a high-throughput, multiplexed, and microfluidic diagnostic and surveillance platform with panels for respiratory viruses and SARS-CoV-2 variants that can be parallelized to test 300-550 patient specimens in an 8 hour working day. To make mCARMEN a clinically relevant technology, we built on CARMEN v1[40] by streamlining the workflow and incorporating commercially available Fluidigm instrumentation. We validated mCARMEN on 2,881 patient specimens for the detection of 9-21 human respiratory viruses (RVP) or SARS-

CoV-2 variant mutations (VIP) with high concordance to comparator assays which passed the FDA‟s performance criteria for all but one virus. Notably, when testing previously positive clinical specimens, we found a substantial proportion were not positive by concurrent testing, but were positive by mCARMEN. This suggests sample degradation issues - a known problem when detecting RNA viruses in clinical specimens[42,49] - that mCARMEN is more robust to handling than RT-qPCR or NGS. Though we cannot rule out false positives, we did not detect SARS-CoV-2 in specimens prior to the pandemic and we had 100% concordance with true virus-negative specimens.

To enhance mCARMEN‟s clinical diagnostic relevance and meld it with surveillance technology requirements, we further maximized its multiplexing capabilities by discriminating between mutations for variant lineage classification in patient specimens and quantifying viral genomic copies. Currently, variant lineage classification is only evaluated by NGS, which is costly and relies on specialized expertise found outside the clinic[17,19]. VIP gives similarly rich information about key SARS-CoV-2 mutations at 5-10x cheaper, per sample, than NGS, and is far more comprehensive than current nucleic acid-based diagnostics. Importantly, since we routinely design guides to preemptively identify mutations of interest in the spike gene in preparation for emerging variants, VIP was poised to differentiate Omicron immediately. VIP allowed us to identify the rapid emergence of Omicron in Massachusetts ~8 days before NGS and provided us specificity, unlike the widely used Spike Gene Target Failure (SGTF) of RT-PCR. Given the number of mutations detected by VIP, we expect to observe distinct mutation signatures between variant lineages that will allow us to differentiate these and future variants of concern from each other without assay redesign.

We also adapted mCARMEN for dual Cas12 and Cas13 detection by capitalizing on the differing protein kinetics. A few groups have studied Cas12 and Cas13 reaction kinetics to inform assay quantification[50,51], but the range of concentrations being quantified has been limited due to reaction saturation. We expanded the quantifiable concentration range to 5-6 orders of magnitude, which is similar to RT-qPCR. These mCARMEN applications have the potential to provide a more holistic diagnosis to the patient, but validation on patient samples is needed.

We rapidly developed mCARMEN for use in the COVID-19 pandemic, but faced challenges during the clinical validation and approval process needed for a large-scale roll-out. Specifically, it was difficult to obtain at least 30 previously confirmed clinical specimens for each virus on RVP with enough material available for extensive concurrent testing, while also facing specimen degradation issues that inevitably occur over time. Although our findings indicate that mCARMEN‟s performance exceeds the FDA‟s requirements for emergency use authorization (EUA), such authorization has not yet been granted.

Further work will be required to bring mCARMEN fully to the clinic, such as obtaining FDA approval, integrating RVP and VIP into a single panel, decreasing the amount of manual labor and easing Fluidigm equipment constraints. Nonetheless, we have taken substantial steps to streamline the assay workflow while enhancing sensitivity without sacrificing specificity. By combining high-throughput, multiplexed pathogen testing with variant tracking, the mCARMEN platform is highly scalable and amenable to clinical laboratory settings for the detection of respiratory pathogens and variants. This technology also has the potential to test for other types of infectious disease[52] and can be used on other sample types[40,53] to achieve even more comprehensive diagnostic and surveillance capabilities.

Figure 1. Implementation of CARMEN using a microfluidic system improves sensitivity and speed. a, Schematic of CARMEN v1 (top) and mCARMEN (bottom) workflows. **b**, Heatmap showing mCARMEN fluorescent data across 21 human respiratory viruses (synthetic DNA fragments and corresponding viral Cas13 crRNAs) that were serially diluted from 103-101 copies/µL and amplified using two separate primer pools. All samples were background subtracted from the NTC-noMg negative control. **c**, Concordance between CARMEN v1 and mCARMEN from **b**. Blue: targets at 10^3 copies/µL; green: targets at 10^2 copies/µL; red: targets at 10^1 copies/µL. **d**, Fluorescence kinetics of amplified SARS-CoV-2 DNA gene fragments from 10^4-10^1 copies/µL at 0, 60, and 180 minutes post-reaction initiation. Blue: mCARMEN; red: CARMEN v1. **e**, A 21 human respiratory virus panel was tested on clinical specimens from 6 SARS-CoV-2 positive, 4 SARS-CoV-2 negative NP swabs, and 8 FLUAV positive specimens, collected prior to Dec. 2019, and 5 no target controls (NTCs). The heatmap shows fluorescent signals from SARS-CoV-2 crRNA, FLUAV crRNA and no crRNA control. Blue: mCARMEN; red: CARMEN v1. **f**, Concordance of mCARMEN and NGS on 58 suspected respiratory virus infected patient specimens collected prior to Dec. 2019 shown as a bar graph; overall concordance shown as a confusion matrix. Black: detected by both mCARMEN and NGS; blue: detected by mCARMEN only; green: detected by NGS only. mCARMEN values are shown as the normalized fluorescence signal (FAM/ROX) (FAM signal divided by the signal for the passive reference dye, ROX, at 1 hour post-reaction initiation). CARMEN v1 values are shown as the raw fluorescence signal (FAM) at 3 hours post-reaction initiation. NTC, no target control; NTC-extract, no target control taken through extraction, cDNA synthesis, amplification, and detection; NTC-cDNA, no target control taken through cDNA synthesis, amplification, and detection; NTC-amp, no target control taken through amplification and detection; NTC-det, no target control taken through detection; NTC-noMg, no target control expected to have no fluorescent signal due to lack on Mg2+ needed to activate Cas13.

Figure 2. Evaluation of an automated and condensed mCARMEN workflow. a, Schematic of the streamlined mCARMEN workflow for testing of 188 patient specimens using a panel of 9 human respiratory viruses, RVP (SARS-CoV-2, HCoV-HKU1, HCoV-OC43, HCoV-NL63, FLUAV, FLUBV, HPIV-3, HRSV, HMPV) and a human internal control (RNase P). **b**, Concordance of RVP and RT-qPCR results. Top, RT-qPCR results were obtained from concurrent testing with mCARMEN testing; bottom, RT-qPCR results were obtained from original testing. **c**, Scaled normalized fluorescence at 1 hour post-reaction initiation for 525 NP swabs ranked by increasing SARS-CoV-2 signal (blue); the respective RNase P signal (gray) is also shown. Normalized fluorescence signal (FAM/ROX), (FAM signal divided by the signal for the passive reference dye,, ROX, signal at 1 hour post-reaction initiation)scaled from 0 to 1. NTC-noMg signal was set as 0 and the maximum normalized fluorescence value at 1 hour was set as 1. Dashed horizontal line: threshold for RVP positivity, calculated by multiplying the NTC-extract fluorescence value by 1.8; NTC-extract: no template control taken through the entire workflow. Gray X, the single failed sample excluded from concordance calculations and other analyses. **d**, Scatter plot of the scaled normalized fluorescence values from **b** compared to viral Ct values obtained from concurrent testing with the CDC 2019-nCoV Kit. Green: positive SARS-CoV-2 signal detected by both RVP and RT-qPCR; gray: inconclusive RT-qPCR result indicating that one or two of the three technical replicates were undetermined; black: undetermined RT-qPCR result indicating that all three technical replicates were negative for SARS-CoV-2. Dashed horizontal lines: threshold for RVP positivity. Dashed vertical line: Ct value of 40 (CDC positivity cutoff).

Figure 3. Clinical evaluation of RVP at a CLIA-certified laboratory. a, Workflow for limit of detection (LOD) studies following the FDA guidelines for establishing assay sensitivity. **b**, Fluorescent values for SARS-CoV-2 target LOD at the indicated SARS-CoV-2 concentrations; 20 replicates were performed. **c**, Normalized fluorescence signal for each virus on the RVP using the on-target sequence (Should Detect), closely related sequences (Should Not Detect), and a no target control NTC (see Supplementary Table 2 for sequence information [AU: Correct?]). Should and Should Not Detect activities were based on ADAPT design predictions (see Methods for details). Closest to further relatives are based on percent nucleotide homology to the corresponding on-target sequence. **d**, Positive percent and negative percent agreement (PPA, NPA, respectively) for each virus on the RVP, calculated based on clinical data in Supplementary Table 5. **e**, Concordance of the performance of the RVP to concurrent comparator assays for 166 retrospective patient specimens tested (left) and 150 contrived samples (right).

Figure 4. Viral quantification using both Cas12 and Cas13 in combination. a, Schematic of the procedure for use of both Cas12 and Cas13 for quantification of viral copy number in samples. Fluorescence is plotted over time to determine the IC_{50} value at each concentration using a sigmoidal 4PL fit. The IC_{50} values are then plotted by concentration to generate a semilog line with an R^2 value >0.8 for Cas12 and Cas13 individually. After line generation, the IC_{50} value of each patient sample is plotted onto these lines to determine viral copies/µL. **b**, Normalized fluorescence ratio of Cas13 crRNA (top) and Cas12 crRNA (bottom) signal over time at varying concentrations of synthetic SARS-CoV-2 Orf1ab RNA. **c**, Plots showing semilog lines generated by IC_{50} values from the Cas12 and Cas13 crRNA signals, as well as Ct values from RT-qPCR for >4 target concentrations of SARS-CoV-2 (left) and FLUAV (right) syntheticRNA. Blue: Cas13; Orange: Cas12; Gray: Ct from RT-qPCR. **d**, Comparison of mCARMEN IC_{50} values to RT-qPCR Ct values using linear regression, with the best line fit shown as a dashed line. Black: SARS-CoV-2; Gray: FLUAV.

Figure 5. SARS-CoV-2 variant identification using SNP-determining Cas13 crRNA combinations. a, Schematic of procedure for the mCARMEN variant identification panel (VIP). The entire SARS-CoV-2 spike gene is amplified to detect the presence of a mutation by differentiating between the ancestral, no mutation, sequence or the derived, mutation-containing, sequence with highly specific Cas13 crRNAs. **b**, SARS-CoV-2 viral seed stocks from ancestral (WA), Alpha, Beta, Gamma, Delta, or Epsilon variant lineages (10^6 copies/mL) were amplified by 2 primer pairs and tested for the presence or absence of spike gene mutations. Data are shown as the $\log_2$ of the maximum crRNA fluorescence ratio at any time point up to 180 minutes post-reaction initiation. Log2 fluorescence ratios were calculated by (-1)*ancestral/mutation or mutation/ancestral representing either the presence of the ancestral sequence (blue) or the derived sequence (purple), respectively. * indicates that the particular mutation was confirmed by NGS. **c**, Comparison of the performance of and NGS on 106 SARS-CoV-2-positive variant patient specimens, based on the final variant call as assessed by unique combinations of mutations (see Methods for details). Black: variant correctly identified by both VIP and NGS; Yellow: NGS only; Green: VIP only. **d**, Plot showing the $\log_2$ maximum crRNA fluorescence ratio of mutation/ancestral (positive, derived) or ancestral/mutation (negative, ancestral) at any time point up to 180 minutes post-reaction initiation for 106 variant patient specimens tested for various SNPs by VIP. Patient specimens are classified as Alpha (purple), Beta (blue), Gamma (teal), Delta (green), or Epsilon (yellow) based on a combination of mutations expected for that variant lineage. **e**, Analysis of how VIP compares to NGS for the 106 variant patient specimens. Black: mutation correctly identified by both VIP and NGS; Yellow: NGS only; Green: VIP only; Gray: ancestral for VIP and NGS.

Figure 6. Rapid and specific identification of the Omicron variant using mCARMEN VIP. a, Expected mutations across 6 SARS-CoV-2 variant lineages (Alpha, Beta, Gamma, Delta, Epsilon, Omicron) detectable by VIP. Blue boxes represent the presence of a mutation; white boxes represent the absence of a mutation. **b**, Proportion of Omicron and Delta variant lineages as assessed by VIP in specimens (n=430) collected on December 6-16 at the Harvard University CLIA Laboratory (HUCL). Green: Omicron; Black: Delta. Error bars represent binomial sampling 95% confidence intervals. **c**, Proportion of Omicron and Delta variant lineages as assessed by VIP and NGS in specimens (n=1,557) collected on December 13-22 from throughout the state of Massachusetts. Blue: Omicron; Black: Delta; Closed circles: mCARMEN; Open circles: NGS. Error bars represent binomial sampling 95% confidence intervals. **d**, Scatter plot of the proportion of Omicron based on the VIP and NGS variant lineage results. The linear regression line fit is shown as a blue line; R^2 = 0.998. MA, Massachusetts. **e**, Comparison of the time delay from specimen extraction to determination of the variant lineage for VIP and NGS. Data represents the proportion of Omicron from specimens collected at HUCL and within the state of Massachusetts. Blue closed circles: VIP MA specimens from c; Blue open circles: NGS MA specimens from **c**; Green: VIP HUCL specimens from **b**.

Author Contributions:

N.L.W., C.M., P.C.B, and P.C.S. initially conceived this study then involved C.M.A., S.G.T., and J.W. for preliminary implementation. N.L.W., M.Z., J.W., C.M.A., S.G.T., M.W.T., J.K. set up 21 respiratory virus testing on CARMEN v1. N.L.W. and S.M. designed the primers and crRNAs for the 21 respiratory viruses tested on CARMEN v1 and mCARMEN. N.L.W., J.W., C.M.A., S.G.T. performed initial experiments on Fluidigm instrumentation. M.Z., J.W., C.M.A. wrote the python scripts for mCARMEN data analysis. N.L.W. performed experiments to streamline the mCARMEN workflow with help from C.H., J.W., and S.G.T. N.L.W., C.H., MM conducted the SARS-CoV-2 patient sample testing in an academic setting, B.L.M. and F.C. helped obtain these samples. C.H., E.M.M., B.M.S., J.E., D.B., G.M. performed clinical evaluation of mCARMEN RVP at MGH, under guidance from N.L.W., J.J., J.E.L., E.R., J.A.B., C.M. J.W. wrote and generated the software used for RVP. N.L.W. with help from M.R.B. conducted NGS on patient samples. N.L.W. designed and tested the primers for VIP, and N.L.W. and S.M. designed the crRNAs for VIP. N.L.W. conducted the experimental validation of VIP. M.K.K., M.W.W., M.W.K., and J.R.B. provided FLUAV samples, SARS-CoV-2 VOC seed stocks, and SARS-CoV-2 VOC patient samples and the corresponding NGS data. K.J.S., N.A.F., B.A.P., G.L.G. provided assistance in patient sample collection and associated IRBs. N.L.W. tested all SARS-CoV-2 Alpha-Delta samples by mCARMEN. M.Z. wrote and generated the variant calling analysis pipeline for VIP testing under guidance from N.L.W. N.L.W., T.G.N., and M.R.B. tested all Omicron samples by mCARMEN with analysis help from G.K.M., L.A.K., D.J.P. N.L.W. conducted experiments to make mCARMEN quantitative with assistance from T.G.N. K.J.S., M.J.S., S.B.G., G.R.G., S.S., L.C.M., C.M.B., D.J.P., B.L.M., C.T.H., D.T.H., J.E.L., J.R.B., E.R., J.A.B., P.C.B., P.C.S., C.M. provided insights into the work overall. N.L.W. generated the figures with help from M.Z. and J.W. N.L.W. wrote the paper with help from C.H. and guidance from P.C.S. and C.M. J.A.B., P.C.B., P.C.S., and C.M. jointly supervised the work. All authors reviewed the manuscript.

Acknowledgements:

We would like to thank the Blainey Lab and Hung Lab at the Broad Institute for providing additional laboratory space to perform the work; J. Arizti Sanz, Y. Zhang, and A. Bradley for helping with guide design or sharing reagents; G. Adams, S. Dobbins, S. Slack, K. DeRuff and other members of the Sabeti Lab COVID-19 sequencing team for providing patient samples; K. Carpenter-Azevedo from RIDOH for organizing and sending Rhode Island patient samples; C.

Tomkins-Tinch, C. Loreth, and other Sabeti Lab members for providing assistance with NGS analysis on Terra; B. Zhou for helping provide the SARS-CoV-2 VOC seed stocks and patient samples; H. Metsky, C. Freije, J. Arizti Sanz, S. Siddiqui for their thoughtful discussions and reading of the manuscript; Anonymous reviewers for providing great insights into the work. We would also like to acknowledge all members of the Massachusetts Department of Public Health, Broad Institute SARS-CoV-2 Genomics and Data Science Platforms, and Rhode Island Department of Public Health.

Funding was provided by DARPA D18AC00006. This work is made possible by support from Flu lab and a cohort of generous donors through TED‟s Audacious Project, including The ELMA Foundation, MacKenzie Scott, the Skoll Foundation, and Open Philanthropy. Funding for NGS was provided by Centers for Disease Control and Prevention COVID-19 baseline genomic surveillance contract sequencing (75D30121C10501 to Clinical Research Sequencing Platform, LLC), a CDC Broad Agency Announcement (75D30120C09605 to B.L.M), National Institute of Allergy and Infectious Diseases (U19AI110818 and U01AI151812 to P.C.S.). M.Z. and M.W.T. were supported by the National Science Foundation Graduate Research Fellowship under Grant No. 1745302. B.A.P. is supported by the National Institute of General Medical Sciences grant T32GM007753. P.C.S. is supported by the Howard Hughes Medical Institute and the Merck KGaA Future Insight Prize. C.M. is supported by start-up funds from Princeton University.

Competing Interests Statement

N.L.W., S.G.T., C.M.A., D.T.H., P.C.B., P.C.S., and C.M. are co-inventors on a patent related to this work. P.C.B is a co-inventor on patent applications concerning droplet array technologies and serves as a consultant and equity holder of companies in the microfluidics and life sciences industries, including 10x Genomics, GALT, Celsius Therapeutics, Next Generation Diagnostics, Cache DNA, and Concerto Biosciences; P.C.B‟s laboratory receives funding from industry for unrelated work. J.A.B. has received research support for other studies from Pfizer, Zeus, bioMerieux, Immunetics, Alere, Diasorin, and the Bay Area Lyme Foundation (BALF). P.C.S. is a co-founder of and consultant to Sherlock Biosciences and a Board Member of Danaher Corporation, and holds equity in the companies. The remaining authors declare no competing interests.

Code availability

The code used for data analysis in this study is made available on Github: https://github.com/broadinstitute/mcarmen.

Data availability

All requests for raw and analyzed data and materials will be reviewed by the Broad Institute of Harvard and MIT to verify if the request is subject to any intellectual property or confidentiality obligations. Data and materials that can be shared will be released via a Material Transfer Agreement. RNA sequencing data have been deposited to the Sequence Read Archive under the BioProject Accession code: PRJNA802370 and will be made available upon request for academic use and within the limitations of the provided informed consent by the corresponding author upon acceptance. Source code is available on github: https://github.com/broadinstitute/mcarmen.

Reporting summary

Further information on research design is available in the Nature Research Reporting Summary linking to this article.

Methods

Patient samples / ethics statement

Use of clinical excess of human specimens from patients with SARS-CoV-2 from the Broad Institute"s Genomics Platform CLIA Laboratory was approved by the MIT IRB Protocol #1612793224. Additional SARS-CoV-2 samples were collected from consented individuals under Harvard Longwood Campus IRB #20-1877 and covered by an exempt determination (EX-7295) at the Broad Institute. Other human-derived samples from patients with SARS-CoV-2 were collected by the CDC and determined to be non-human subjects research; the Broad Office of Research Subject Protections determined these samples to be exempt (EX-7209). Human specimens from patients with SARS-CoV-2, HCoV-HKU1, HCoV-NL63, FLUAV, FLUBV, HRSV, and HMPV were obtained under a waiver of consent from the Mass General Brigham IRB Protocol #2019P003305. Researchers at Princeton were determined to be conducting not-engaged human subjects research by the Princeton University IRB.

We gratefully acknowledge the personnel at Rhode Island Department of Public Health for the samples they provided, in particular: Ewa King, Ph.D., Associate Director of Health, and Richard C. Huard, Ph.D., D(ABMM), Chief Clinical Laboratory Scientist, both at the Division of State Laboratories and Medical Examiner at Rhode Island Department of Health.

General mCARMEN Procedures

Detailed description of running mCARMEN RVP as a standard operating procedure (SOP) can be found as Supplementary Note 1.

Preparation and handling of synthetic materials

crRNAs were synthesized by Integrated DNA Technologies (Coralville, IA), resuspended in nuclease-free water to 100 μM, and further diluted for input into the detection reaction. Primer sequences were ordered from Eton or Integrated DNA Technologies, resuspended in nuclease-free water to 100 μM, and further combined at varying concentrations for pooled amplification.

Preparation of *in vitro* transcribed (IVT) material

DNA targets were ordered from Integrated DNA Technologies and *in vitro* transcribed (IVT) using the HiScribe T7 High Yield RNA Synthesis Kit (New England Biolabs, NEB).

Transcriptions were performed according to the manufacturer"s recommendations with a reaction volume of 20 µL that was incubated overnight at 37°C. The transcribed RNA products were purified using RNAClean XP beads (Beckman Coulter) and quantified using NanoDrop One (Thermo Scientific). Depending on the experiment, the RNA was serially diluted from 10^{11} down to 10^{-3} copies/µL and used as input into the amplification reaction.

Extraction - Manual or Automated

RNA was manually extracted from input material using the QIAamp Viral RNA Mini Kit (QIAGEN) according to the manufacturer's instructions. RNA was extracted from 140 µL of input material with carrier RNA and samples were eluted in 60 µL of nuclease free water and stored at −80 °C until use.RNA was automatically extracted using the MagMAX™ DNA Multi-Sample Ultra 2.0 Kit on a KingFisher™ Flex Magnetic Particle Processor with 96 Deep-Well Head (Thermo Fisher Scientific). RNA was extracted from 200 µL of input material and was run according to the “Extract RNA - Automated method (200-µL sample input volume)” protocol in TaqPath™ COVID-19 Combo Kit Protocol, on page 21-24. The MVP_2Wash_200_Flex protocol was used. Samples were eluted in 50 µL of elution solution and either directly added to the amplification reaction or stored at −80°C until use.

Amplification: Qiagen or SSIV

We followed the CARMEN v1 platform for two-step reverse transcription amplification then transitioned to a single-step amplification reaction after experiments depicted in Figure 1. We used the Qiagen OneStep RT-PCR Mix for Figures 2,3,5 and Invitrogen SuperScript IV One-Step RT-PCR System for Figure 4. For the Qiagen OneStep RT-PCR, a total reaction volume of 50 µL was used with some modifications to the manufacturers recommended reagent volumes. Specifically 1.25X final concentration of OneStep RT-PCR Buffer, 2x more Qiagen Enzyme Mix, and 20% RNA input. Final concentrations for all viral primers were 300 nM and 100 nM for RNase P primers. The following thermal cycling conditions were used: (1) reverse transcription at 50°C for 30 min; (2) initial PCR activation at 95°C for 15 min; (3) 40 cycles of 94°C for 30 s, 58°C for 30 s, and 72 °C for 30 s. For Invitrogen SuperScript IV One-Step RT-PCR, a total reaction volume of 25 µL with 20% RNA input and final primer concentrations at 1 µM. The following thermal cycling conditions were used: (1) reverse transcription at 50°C for 10 min; (2) initial PCR activation at 98°C for 2 min; (3) 35 cycles of 98°C for 10 s, 60°C for 10 s, and 72 °C for 1 min 30 s; (4) final extension at 72 °C for 5 min. See Supplementary Table 4 for information on primer sequences used in each mCARMEN panel.

Fluidigm Detection

The Cas13 detection reactions were made into two separate mixes: assay mix and sample mix, for loading onto a microfluidic IFC (depending on the experiment, either Gene Expression (GE) or Genotyping (GT) IFCs were used in either a 96.96 or 192.24 format) (Fluidigm):
The *assay mix* contained LwaCas13a (GenScript) and on occasion LbaCas12a (NEB) concentration varied with experiment, 1× Assay Loading Reagent (Fluidigm), 69U T7 polymerase mix (Lucigen), and crRNA concentration varied with experiment for a total volume of 16 µL per reaction. See below for details pertaining to each mCARMEN panel.
The *sample mix* contained 25.2U RNase Inhibitor (NEB), 1× ROX Reference Dye (Invitrogen), 1× GE Sample Loading Reagent (Fluidigm), 1 mM ATP, 1 mM GTP, 1 mM UTP, 1 mM CTP, 9 mM $MgCl_2$ in a nuclease assay buffer (40 mM Tris-HCl pH 7.5, 1 mM DTT) and either a 500 nM quenched synthetic fluorescent RNA reporter (FAM/rUrUrUrUrUrU/3IABkFQ/ or VIC/rTrTrArTrTrArTrT/3IABkFQ/ Integrated DNA Technologies) or RNaseAlert v2 (Invitrogen) was used for a total volume of 12.6 µL. See below for details on each mCARMEN panel.

IFC Loading and Run: Syringe, Actuation Fluid, Pressure Fluid (Fluidigm), and 4 µL of assay or sample mixtures were loaded into their respective locations on a microfluidic IFC (depending on the experiment, either Gene Expression (GE) or Genotyping (GT) IFCs were used in either a 96.96 or 192.24 format) and were run according to the manufacturer‟s instructions. The IFC was loaded onto the IFC Controller RX or Juno (Fluidigm) where the „Load Mix‟ script was run. After proper IFC loading, images over either a 1-3 hour period were collected using a custom protocol on Fluidigm‟s EP1 or Biomark HD.

Fluidigm Data Analysis

We plotted reference-normalized background-subtracted fluorescence for guide-target pairs. For a guide-target pair (at a given time point, t, and target concentration), we first computed the reference-normalized value as (median(P_t-P_0)/(R_t-R_0)) where P_t is the guide signal (FAM) at the time point, P_0 is its background measurement before the reaction, R_t is the reference signal (ROX) at the time point, R_0 is its background measurement, and the median is taken across replicates. We performed the same calculation for the no template (NTC) control of the guide, providing a background fluorescence value for the guide at t (when there were multiple technical replicates of such controls, we took the mean value across them). The reference-normalized background-subtracted fluorescence for a guide-target pair is the difference between these two values.

21 Respiratory Viruses (Fig. 1)

Design

The oligonucleotide primers and CRISPR RNA guides (crRNAs) are designed for detection of conserved regions of the following respiratory viruses: SARS-CoV-2, HCoV-229E, HCoV-HKU1, HCoV-NL63, HCoV-OC43, FLUAV, FLUBV, HMPV, HRSV, HPIV-1,2,3,4, AdV, HEV-A,B,C,D, SARS-CoV, MERS-CoV, and HRV. More specifically, complete genomes for all viruses on the panel were downloaded from NCBI and aligned using MAFFT[54]. For viral species with fewer than 1000 sequences, MAFFT‟s „FFT-NS-ix1000‟ algorithm was used. For viral species with >1000 sequences, MAFFT‟s „FFT-NS-1‟ algorithm was used. These aligned sequences were then fed into ADAPT for crRNA design with high coverage using the „minimize guides‟ objective (>90% of sequences detected). Once highly conserved regions of the viral genome were selected with ADAPT for optimal guide design, primers were manually designed to amplify a 100-250 bp target region with the crRNA predicted to bind in the middle of the fragment. ADAPT‟s constraints on primer specificity were relaxed and in some cases multiple primers were needed to encompass the full genomic diversity of a particular virus species. For optimal amplification, the primers were split into two pools. These primer pools and crRNA sequences are listed in Supplementary Table 4.

Target control - PIC1 and PIC2

The consensus sequences generated directly above after multiple genome alignment with MAFFT were used to order a 500 bp dsDNA fragment encompassing the primer and crRNA binding sites. RNA was generated following the method described in „General mCARMEN Procedure - Preparation of IVT Material‟ and diluted to 10^6 copies/µL in pools based on the primer pools mentioned above (PIC1, PIC2). The PICs were used as input into the CARMEN v1 or mCARMEN detection reaction to function as a detection positive control.

Sample Extraction: Manual or Automated

Automated and manual extraction was performed according to methods described under „General mCARMEN Procedures - Extraction‟

Amplification: Two-Step

We followed the CARMEN v1 platform for two-step reverse transcription amplification, which was performed first by cDNA synthesis and then by PCR.

cDNA synthesis using SSIV

10 µL of extracted RNA was converted into single-stranded cDNA in a 40 µL reaction. First, Random Hexamer Primers (ThermoFisher) were annealed to sample RNA at 70°C for 7 min, followed by reverse transcription using SuperScript IV (Invitrogen) for 20 min at 55°C. cDNA was stored at −20°C until use. DNase treatment was not performed at any point during sample preparation.

Q5 DNA amplification

Nucleic acid amplification was performed via PCR using Q5 Hot Start polymerase (NEB) using primer pools (with 150 nM of each primer) in 20 µL reactions. Amplified samples were added directly into the detection reaction or stored at −20°C until use. The following thermal cycling conditions were used: (1) initial denaturation at 98°C for 2 min; (2) 45 cycles of 98°C for 15 s, 50°C for 30 s, and 72°C for 30 s; (3) final extension at 72°C for 2 min. Each target was amplified with its corresponding primer pool, as listed under „oligonucleotides used in this study."

Detection

CARMEN-Droplet

For colour coding, unless specified otherwise, amplified samples were diluted 1:10 into nuclease-free water supplemented with 13.2 mM $MgCl_2$ prior to colour coding to achieve a final concentration of 6 mM after droplet merging. Detection mixes were not diluted. Colour code stocks (2 µL) were arrayed in 96W plates (for detailed information on construction of colour codes, see „Colour code design, construction and characterization"). Each amplified sample or detection mix (18 µL) was added to a distinct colour code and mixed by pipetting.

For emulsification, the colour-coded reagents (20 µL) and 2% 008-fluorosurfactant (RAN Biotechnologies) in fluorous oil (3M 7500, 70 µL) were added to a droplet generator cartridge (Bio Rad), and reagents were emulsified into droplets using a Bio Rad QX200 droplet generator or a custom aluminum pressure manifold.

For droplet pooling, a total droplet pool volume of 150 µL of droplets was used to load each standard chip; a total of 800 µL of droplets was used to load each mChip. To maximize the probability of forming productive droplet pairings (amplified sample droplet + detection reagent droplet), half the total droplet pool volume was devoted to target droplets and half to detection reagent droplets. For pooling, individual droplet mixes were arrayed in 96W plates. A multichannel pipette was used to transfer the requisite volumes of each droplet type into a single row of eight droplet pools, which were further combined to make a single droplet pool. The final droplet pool was pipetted up and down gently to fully randomize the arrangement of the droplets in the pool. The pooling step is rapid (<10 min), and small molecule exchange between droplets during this period does not substantially alter the colour codes.

mCARMEN

We followed the methods under General CARMEN Procedures - Detection - Fluidigm detection with the following modifications: 42.5 nM LwaCas13 and 212.5 nM crRNA in each assay mix reaction, and 500 nM RNaseAlert v2 in each sample mix reaction.

Data Analysis

CARMEN v1

We followed the data analysis pipeline from CARMEN v1[40] to demultiplex and readout the fluorescence intensity of the reporter channel for each droplet reaction performed (MatLab 2013). In brief, pre-merge imaging data was processed using custom Python3 scripts to detect fluorescently-encoded droplets in microwells and identify their inputs based on their fluorescence intensity in three encoding channels, 647 nm, 594 nm, and 555 nm. Subsequently, post-merge imaging data was analyzed to extract the reporter signal of the assay in the 488 nm channel, and those reporter fluorescence intensities were physically mapped to the contents of each microwell. Quality control filtering was performed based on the appropriate size of a merged droplet from two input droplets and the closeness of a droplet"s color code to its assigned color code cluster centroid. The median and standard error were extracted from the replicates of all assay combinations generated on the array.

mCARMEN

We followed the methods under „General CARMEN Procedures - Fluidigm Data Analysis" and further visualized the data using Python3, R 4, and Prism 9.

Single-step amplification troubleshooting

The following RT-PCR kits were tested to determine the best performing assay: (1) OneStep RT-PCR Kit (Qiagen) (2) TaqPath™ 1-Step Multiplex Master Mix (Thermo Fisher), (3) One Step PrimeScript™ RT-PCR Kit (Takara), (4) GoTaq® Probe RT-qPCR Kit (Promega), (5) UltraPlex™ 1-Step ToughMix® (4X) (Quantbio), (6) iTaq™ Universal One-Step Kits for RT-PCR (Bio-Rad). Of the kits tested, the OneStep RT-PCR Kit (Qiagen) was chosen for the final mCARMEN protocol.

OneStep RT-PCR Kit (Qiagen)

All or a combination of the following thermal cycling condition ranges were tested to shorten assay run-time: reverse-transcription at 50 °C at 15-30 min, PCR activation at 95 °C at 5-15 min, denaturation step at 94 °C at 10-30 s, and extension step at 72 °C for 10 s to 1 min. The final extension at 72 °C for 10 min was omitted in all runs. The following primer pool conditions were also tested to optimize the assay: 150 nM, 300 nM, 500 nM, and 600 nM of virus-specific primer and 100 nM and 150 nM of RNaseP primers, with 5 µM of each virus-specific primer and 1.7 µM of RNaseP primers. Reaction volumes tested include: 20 µL with 10% RNA template input, 30 µL with 20% RNA template input, and 50 µL with 20% RNA template input. The final amplification conditions used for the RVP panel are described under „General mCARMEN Procedures - Amplification".

TaqPath™ 1-Step Multiplex Master Mix Kit (Thermo Fisher)

The TaqPath™ 1-Step Multiplex Master Mix Kit (Thermo Fisher) was used to amplify nucleic acid according to the manufacturer's instructions, using custom primer pools in 20 µL reactions. Primer pools of 150 nM, 300 nM, and 500 nM and anneal temperatures of 58 °C and 60 °C and were all tested and compared to determine optimal conditions. The following thermal cycling conditions were used: (1) UNG passive reference incubation at 25 °C for 2 min; (2) reverse-transcription incubation at 50 °C for 15 min; (3) enzyme activation at 95 °C for 2 min (4) 40 cycles of 95 °C for 3 s and 60 °C for 30 s. Amplified samples were directly added into the detection reaction or stored at −20 °C until use.

GoTaq® Probe RT-qPCR Kit (Promega)

The GoTaq® Probe RT-qPCR Kit (Promega) was used to amplify nucleic acid via RT-PCR according to the manufacturer's instructions, using custom primer pools in 20 µL reactions. Primer pools of 200 nM, 300 nM, and 500 nM were tested and compared to determine optimal conditions. Each target in the panel was amplified with its corresponding primer pool. The

following thermal cycling conditions were used: (1) reverse-transcription at 45 °C for 15 min and 95 °C for 2 min; (2) 40 cycles of 95 °C for 15 s, 60 °C for 1 min. Amplified samples were directly added into the detection reaction or stored at −20 °C until use.

UltraPlex™ 1-Step ToughMix® (4X) (Quantbio)
The UltraPlex™ 1-Step ToughMix® (4X) (Quantbio) was used to amplify nucleic acid via RT-PCR according to the manufacturer's instructions, using custom primer pools in 20 µL reactions. Primer pools of 200 nM, 300 nM, and 500 nM were tested and compared to determine optimal conditions. Each target in the panel was amplified with its corresponding primer pool. The following thermal cycling conditions were used: (1) reverse-transcription at 50 °C for 10 min and 95 °C for 3 min; (2) 45 cycles of 95 °C for 10 s, 60 °C for 1 min. Amplified samples were directly added into the detection reaction or stored at −20 °C until use.

RVP Testing at Broad research laboratory (Fig. 2)
Design of 9-virus respiratory panel and RNase P
We designed this panel according to the methods described above under „Respiratory Panel - Design" for these 9 viruses: SARS-CoV-2, HCoV-HKU1, HCoV-OC43, HCoV-NL63, FLUAV, FLUAV-g4, FLUBV, HPIV-3, HRSV, and HMPV, with the addition of an RNase P primer pair and crRNA. RNase P primers and crRNAs were designed within the same region of the gene as the CDC RT-qPCR assay (Supplementary Table 4).

Patient Specimen Validation
All patient specimens evaluated on RVP were additionally evaluated concurrently with the CDC 2019-nCoV Real-Time RT-PCR Diagnostic Panel for N1 and RNase P. A subset of specimens were selected for further study using Next Generation Sequencing.

The CDC 2019-nCoV EUA recommends a Ct cutoff of <40 for RNase P and/or SARS-CoV-2. There were 8 specimens that failed quality control metrics and were therefore removed from further analysis in the paper. 5 specimens were previously positive and 3 were negative by prior RT-PCR testing done by the Broad Genomics Platform.

Of the 525 patient specimens evaluated by mCARMEN only two specimens had no detectable levels of RNase P above threshold, one of which was positive for SARS-CoV-2 while the other was virus-negative. The RNase P negative, but virus-positive, specimen likely has a high concentration of viral RNA, which sequesters amplification materials during the reaction, limiting RNase P amplification. The double negative specimen suggests possible extraction failure or sample integrity issues and was thus excluded from further analysis.

RVP Detection
Specimen preparation was performed according to the method outlined in 'General mCARMEN Procedures - Sample Extraction" with 200 µL of input material. Amplification was performed according to methods outlined in 'General mCARMEN Procedures - Amplification" Detection reactions were prepared as described in „General mCARMEN Procedures - Detection" with the following modifications: 42.5 nM LwaCas13 and 212.5 nM crRNA in each assay mix reaction, and 500 nM quenched synthetic fluorescent RNA reporter (FAM/rUrUrUrUrUrU/3IABkFQ/) in each sample mix reaction. Results were analyzed following methods outlined under „General mCARMEN Procedures - Data Analysis".

CDC 2019-nCoV Real-Time RT-PCR Diagnostic Panel - Research Use Only
The CDC 2019-nCoV Real-Time RT-PCR Diagnostic Panel was performed using TaqPath 1-Step RT-qPCR Master Mix (Thermo Fisher) with 1 µL template RNA of either SARS-CoV-2 or

RNase P in 10 µL reactions, run in triplicate. Primers from the 2019-nCoV RUO Kit (IDT) were used. For SARS-CoV-2 a primer pool at 800 µM and probe at 200 µM was used. For RNaseP, a primer pool at 500 µM and a probe at 125 µM was used. The following thermal cycling conditions were used: (1) enzyme activation at 25 °C for 2 min; (2) reverse-transcription at 50 °C for 15 min; (3) PCR activation at 95 °C for 2 min; (4) 45 cycles of 95 °C for 3 s and 55 °C for 30 s. Standard curves were made with spike-in of RNA template (SARS-CoV-2 and RNaseP) to make a ten-fold serial dilution from 10^0 to 10^6 copies/µL. This was run on the QuantStudio™ 6 Flex System.

Next Generation Sequencing

Metagenomic sequencing libraries were generated as previously described[5,55]. Briefly, extracted RNA was DNase treated to remove residual DNA then human rRNA was depleted. cDNA was synthesized using random hexamer primers. Sequencing libraries were prepared with Illumina Nextera XT DNA library kit and sequence with 100-nucleotide or 150-nucleotide paired-end reads. Data analysis was conducted on the Terra platform (app.terra.bio); all workflows are publicly available on the Dockstore Tool Registry Service. Samples were demultiplexed using demux_plus to filter out known sequencing contaminants. Viral genomes were assembled using assemble_refbased, discordant specimens with viral genomes were assembled using assemble_denovo and additionally visualized using classify_kraken, blastn, blastx, geneious, and R. A virus was determined to be present if more than 10 reads mapped to a particular viral genome. Full genomes were deposited into GenBank (BioProject Accession # PRJNA802370).

Clinical Evaluation of RVP in CLIA-certified laboratory at MGH (Fig. 3)

Design

We designed this panel according to the methods described above under „RVP Testing at Broad - Design".

Controls

Automated Extraction, KingFisher Control: Extraction Negative Control (EC) is an RNA extraction control and is prepared by adding 200 µL pooled human sample (negative for all viruses on the panel) to a well with 280 µL of binding bead mix (preparation described in 'Automated Extraction, KingFisher'). The EC should yield a positive result for the RNaseP crRNA and primer pair and a negative result for all other targets.

Nucleic acid amplification controls: No Template Control (NTC) is a negative control for nucleic acid amplification and is prepared by adding 10 µL nuclease-free water (instead of RNA) into 40 µL of OneStep RT-PCR Kit (Qiagen) mastermix. This should yield a negative result for all targets on the panel. *Combined Positive Control (CPC)* is a positive control for nucleic acid amplification and is prepared by pooling *in vitro* transcribed synthetic RNA of all the targets on the panel to 10^3 copy/µL. 11 µL aliquots of this mix are stored at -80°C until use, when 10 µL are added to 40 µL of OneStep RT-PCR Kit (Qiagen) mastermix. This should yield a positive result for all targets on the panel.

Cas13-Detection Controls: Negative Detection Control (NDC) is a negative control for the Fluidigm-detection step and is prepared by adding nuclease-free water (instead of amplified RNA) to the sample mix without $MgCl_2$. This should yield a negative result for all targets on the panel. *No crRNA control (no-crRNA)* is a negative control for the Fluidigm-detection step and is prepared by adding nuclease-free water (instead of 1 µM crRNA) to the assay mix. This should yield a negative result for all targets on the panel.

Batch preparation of sample and assay mixtures

Sample and assay mixtures can be prepared in advance for multiple 96-sample batches following similar methods, with the following changes: the batch sample mix contained all reagents described above, excluding 9 mM $MgCl_2$, and the batch assay mix contained all reagents described above, excluding 2x Assay Loading Reagent. Both mixtures were calculated with 10% overage. Both mixtures were stored at −80 °C until use. 9 mM $MgCl_2$ was added to the sample mix and 2x Assay Loading Reagent was added to each assay mix before use.

SYBR RT-qPCR of viral seed stock and genomic RNA from ATCC and BEI Resources

Quantification of all viral seed stock and genomic RNA received from ATCC and BEI resources was performed using the Power SYBR Green RNA-to-Ct 1-Step Kit (ThermoFisher). Reactions were run in triplicate with 1 µL RNA input in 10 µL reactions. A primer mix at 500nM was used, and all primer sequences used are listed in Supplementary Table 4. The following thermal cycling conditions were used: (1) reverse transcription at 48 °C for 30 min; (2) enzyme activation at 95 °C for 10 min; (3) 40 cycles of 95 °C for 15 s and 60 °C for 1 min; (4) melt curve of 95 °C for 15 s, 60 °C for 15 s, and 95 °C for 15 s. Standard curves were made with spike-in of RNA template to make a ten-fold serial dilution from 10^0 to 10^6 copies/µL. This was run on the QuantStudio™ 6 Flex System.

Limit of Detection (LOD)

Samples were prepared for the LOD experiments using either quantified viral isolates, genomic RNA or IVT partial gene fragments. For the SARS-CoV-2, HCoV-OC43, HRSV, and HPIV-3 assays, quantified viral isolates of known titer (RNA copies/µL) spiked into pooled negative human sample (negative for all viruses on the panel) in Universal Transport Media (UTM), to mimic clinical specimen. The pooled human negative samples were incubated in the binding bead mix solution according to the methods described in „General mCARMEN Procedures - Extraction - Automated." Since no quantified virus isolates for HCoV-NL63, HCoV-HKU-1, FLUAV, FLUAV-g4, FLUBV, and HMPV were available for use at the time the study was conducted, assays designed for RNA detection of these viruses were tested with either genomic RNA from ATCC (FLUAV: cat# NR-43756; FLUBV: cat# VR-1804) or IVT RNA of known titer were spiked into pooled negative human samples in UTM.

RNA was extracted from 200 µL of input material using the MagMAX™ DNA Multi-Sample Ultra 2.0 Kit on a KingFisher™ Flex Magnetic Particle Processor with 96 Deep-Well Head (Thermo Fisher Scientific). This was run according to the protocol listed in TaqPath™ COVID-19 Combo Kit Protocol under "KingFisher, "Extract RNA - Automated method (200 µL input volume)" with the following differences: To prepare the binding bead mix, the following was added: 265 µL binding solution, 10 µL total nucleic acid magnetic beads, 5 µL Proteinase K with 10% overage for multiple samples. 280 µL of the binding bead mix was added to each sample well. The 200 µL of input material includes negative human sample and RNA: 160 µL of pooled human samples (negative for all viruses on the panel) was added to each sample well and incubated for 20 minutes before 40 µL of RNA was spiked in. Samples were eluted in 50 µl of elution solution and either directly added to the amplification reaction or stored at −80 °C until use.

A preliminary LOD for each assay was determined by testing triplicates of RNA purified using the extraction method described in 'RVP panel'. The approximate LOD was identified by extraction, amplification, and detection of 10-fold serial dilutions of IVT RNA of known titer (copies/µL) for 5 replicates. These concentrations ranged from 1e4-1e-3 copies/µL. The lower

bound of the LOD range was determined as the lowest concentration where 5/5 replicates were positive, and the upper bound was determined as the concentration 10-fold above the lower bound.

A confirmation of the LOD for each assay was determined by testing 20 replicates of RNA, purified using the extraction method described in 'RVP panel'. The approximate LOD was identified by extraction, amplification, and detection of 2-fold serial dilutions of the input sample, quantified viral isolates, genomic RNA or IVT RNA. These concentrations ranged from 20-0.5 copies/µL, depending on the virus. The LOD was determined as the lowest concentration where ≥95% (19/20) of the replicates were positive.

Specificity

In silico analysis - Inclusivity

Inclusivity was tested by performing an *in silico* analysis using all publicly available sequences of all targets on the RVP panel. Complete genomes for all viruses were downloaded from NCBI on April 2, 2021 and aligned using MAFFT v7. For viral species with less than 1000 sequences, the FFT-NS-ix1000 algorithm was used to create the MAFFT alignment. For viral species with >1000 sequences, the FFT-NS-1 algorithm was used to create the MAFFT alignment. The primer and crRNA sequences were then mapped to the aligned viral sequences using a consensus alignment to determine the percent identity (homology) and the number of mismatches. The average homology and mismatches were taken across the total number of sequences evaluated. Please note that mismatches below for crRNA sequences do not take wobble base pairing (G-U pairing) into account. Results are summarized in Supplementary Table 8.

Additionally the SARS-CoV-2 crRNA and primer sequences were tested by NCBI BLAST+ against the nr/nt databases (updated 03/31/2021, N=68965867 sequences analyzed) and the Betacoronavirus database (updated 04/01/2021, N=140760). The search parameters were adjusted to blastn-short for short input sequences. The match and mismatch scores are 1 and -3, respectively. The penalty to create and extend a gap in an alignment is 5 and 2, respectively. Blast results confirmed only perfect matches to SARS-CoV-2.

In silico analysis - Specificity

Complete genomes for all viruses were downloaded from NCBI on April 2, 2021 and aligned using MAFFT. For viral species with less than 1000 sequences, FFT-NS-ix1000 was used. For viral species with >1000 sequences, FFT-NS-1 was used for the MAFFT alignment. The primer and crRNA sequences were then mapped to the aligned viral sequences using a consensus alignment to determine percent identity (homology). The average homology was taken across the panel sequences and the total number of sequences evaluated. Bolded text represents on-target primers/crRNA to the intended viral sequences. Not all sequence combinations were evaluated since whole genome homology between many viruses is significantly less than 80%. All primer and crRNA sequences do not have >80% homology to other, unintended viral or bacterial sequences, making the panel highly specific to particular viruses of interest. More specifically, no in silico cross-reactivity >80% homology between any primers and crRNA sequences on RVP is observed for the following common respiratory flora and other viral pathogens: SARS-CoV-1, HCoV-MERS, Adenovirus, Enterovirus, Rhinovirus, *Chlamydia pneumoniae, Haemophilus influenzae, Legionella pneumophila, Mycobacterium tuberculosis, Streptococcus pneumoniae, Streptococcus pyogenes, Bordetella pertussis, Mycoplasma pneumoniae, Pneumocystis jirovecii, Candida albicans, Pseudomonas aeruginosa,*

Staphylococcus epidermis, Streptococcus salivarius. In silico analysis results are summarized in Supplementary Table 9.

In vitro analysis

Targets were selected for in vitro specificity testing based on closely related viral species with high nucleotide identity. The synthetic DNA targets contain the consensus sequence of a particular virus that is position matched to location the RVP virus of interest targets in the viral genome. Samples were prepared for specificity experiments according to methods described above in „General mCARMEN Procedures - Preparation of IVT material," and samples were serially diluted down to a concentration of 10^6 and 10^5 copies/µL. For all samples prepared for specificity experiments, RNA was extracted from 200 µL of input material using the MagMAX™ DNA Multi-Sample Ultra 2.0 Kit on a KingFisher™ Flex Magnetic Particle Processor. This was run according to the extraction, amplification, and detection methods described above under „RVP Testing at Broad."

Patient Specimen Validation

Specimen preparation prior to extraction

All patient specimens from the MGH Clinical Microbiology Lab were initially reported to be positive for HCoV-HKU1, HCoV-NL63, and HMPV via BioFire FilmArray Respiratory Panel (RP2) or positive for SARS-CoV-2, FLUAV (H3), FLUBV, and HRSV via Xpert® Xpress SARS-CoV-2/Flu/RSV (Cepheid). 200 µL of positive for SARS-CoV-2 were aliquoted as follows: 220 µL for testing using the RVP panel, 220 µL for testing using the TaqPath™ COVID-19 Combo Kit, and all remaining specimens were stored at −80 °C. All negative specimens were aliquoted: 220 µL for RVP panel testing, 220 µL for TaqPath™ COVID-19 Combo Kit testing, 400 µL for BioFire FilmArray Respiratory Panel (RP2) testing, and all remaining specimen was stored at −80 °C. All other specimens were aliquoted: 220 µL for RVP panel testing, 400 µL for BioFire FilmArray Respiratory Panel (RP2) testing, and all remaining specimen was stored at −80 °C.

Preparation of contrived samples prior to extraction

Contrived patient samples of viruses HCoV-HKU1, HCoV-OC43, HCoV-NL63, FLUAV-g4, HPIV-3, and HMPV were prepared by diluting either viral seed stock (HCoV-OC43 and HPIV-3) or template RNA (HCoV-HKU1 and HCoV-NL63). See Supplementary Table 10 for viral seed stock vendor details. The viral seed stock or template RNA is added to non-pooled human specimens (negative for all targets, except RNase P, on the RVP panel) at a concentration 2 times the LOD; the concentrations for these samples ranged from 10^2 to 10^6 copies/µL.

RVP

All materials were extracted, amplified, detected, and analyzed using methods described under „General mCARMEN Procedures " and „RVP Testing at Broad - Patient Specimen Validation."

TaqPath™ COVID-19 Combo Kit

A subset of patient specimens, all SARS-CoV-2 and negative patient specimens, from the MGH Clinical Microbiology Laboratory were verified using the TaqPath™ COVID‑19 Combo Kit (ThermoFisher). These samples were initially reported to be positive for SARS-CoV-2 via Xpert® Xpress SARS-CoV-2/Flu/RSV (Cepheid) or reported to be negative for all targets (excluding RNaseP) on the RVP panel via BioFire FilmArray Respiratory Panel (RP2).The TaqPath™ COVID‑19 Combo Kit was performed according to the manufacturer's instructions. The assay was performed using the Applied Biosystems 7500.

BioFire FilmArray Respiratory Panel (RP2)

A subset of patient specimens from the MGH Clinical Microbiology Laboratory, all HCoV-HKU1, HCoV-NL63, FLUAV (H3), FLUBV, HRSV, HMPV and negative patient specimens, were verified using the BioFire FilmArray Respiratory Panel (RP2) (Biofire Diagnostics). These specimens were either initially reported to be positive for HCoV-HKU1, HCoV-NL63, and HMPV via BioFire FilmArray Respiratory Panel (RP2) or positive for FLUAV (H3), FLUBV, and HRSV via Xpert® Xpress Flu/RSV (Cepheid). For each run, one patient specimens in UTM at 300 µL was verified using the BioFire FilmArray Respiratory Panel (RP2) according to the manufacturer's instructions. Any remaining specimen was stored at -80°C.

Controls for this assay were received with the kit and ready for use. Control 1 is expected to be positive for adenovirus, HMPV, Human Rhino/Enterovirus, FLUAV (H1-2009), FLUAV (H3), HPIV-1, HPIV-2. Control 2 is expected to be positive for HCoV-229E, HCoV-HKU1, HCoV-NL63, HCoV-OC43, FLUAV (H1), FLUBV, HPIV-2, HPIV-3, HRSV.

The results were automatically displayed on the FilmArray software with each target in a run reported as “detected” or “not detected.” If either control fails, the software marks this run as “invalid.” When sufficient human sample volume was available, samples with invalid results were re-run.

Analysis Software

The analysis software comprises python scripts executing the data analysis described in Methods 2h and taking into account the controls described in Methods section 6aii. They are packaged into an executable with graphical user-interface using the Python module Gooey 1.0.7.

In short, the reference-normalized background-subtracted fluorescence is calculated for guide-target pairs for the measurement after 60 min. Then, the dynamic range and the separation band are assessed.

Separation band = (mean of positive controls - 3 standard deviations of positive controls) - (mean of negative controls - 3 standard deviations of negative controls)
Dynamic range = | mean of positive controls - mean of negative controls|

If the ratio of separation band to dynamic range is equal or less than 0.2, the whole assay is invalid. Next, for the positive and negative controls, outliers based on three standard deviations are identified. If a positive control has a too low value or a negative control a too high value, the respective assay is invalid. For the remaining samples, hit calling is performed based on comparing the signal to the water control. If the signal is 1.8x higher than the water control, the guide-target pair is called a hit. Based on this hit calling, the extraction control, the negative and positive detection controls and internal controls are verified. If their result does not correspond to their expected hit status, either the respective assay or specimens is turned invalid. All specimens to be valid need to be either positive for RNase P or at least one other assay. Finally, the software annotates the results as csv files and visualizes them as an annotated heatmap.

Cas13- and Cas12-based detection with mCARMEN (Fig. 4)

Design for Cas12-based detection

Cas13 crRNAs from RVP were utilized. Cas12 crRNAs were manually designed in the same region of the viral genome as the Cas13 crRNAs to reduce the need for additional primer design while maintaining Cas12‟s PAM requirements. Only one additional primer was designed inorder

to properly amplify all targets on RVP. All crRNAs and primers are listed in Supplementary Table 4.

Detection

We followed the methods under „General mCARMEN Procedures - Detection" with the following modifications: 10-60 nM LwaCas13, 10-60 nM LbaCas12a, 125 nM Cas13a crRNA, and 125 nM Cas12 crRNA in each assay mix reaction, and 500 nM quenched synthetic fluorescent RNA reporter (FAM/rUrUrUrUrUrUrU/3IABkFQ/ and VIC/rTrTrArTrTrArTrT/3IABkFQ) in each sample mix reaction.

Data analysis

We generally followed the methods under „General mCARMEN Procedures - Analysis" this time with also taking into account VIC signal separate from FAM signal. We used a custom python script to determine whether the FAM signal of a reaction is significantly above background by comparing it to the no-template control. If the background-subtracted and normalized fluorescence intensity is 1.8 higher than the normalized and background-subtracted no-templated control, the assay is considered positive.

Variant Testing (Fig. 5&6)

Design

The crRNAs for SNP discrimination were designed using a generative sequence design algorithm (manuscript in prep.). This approach uses ADAPT"s predictive model to predict the activity of candidate crRNA sequences against on-target and off-target sequences[35]. These predictions of candidate crRNA activity steer the generative algorithm"s optimization process, in which it seeks to design crRNA probes that have maximal predicted on-target activity and minimal predicted off-target activity. Using this design algorithm, we selected the 26 mutations to detect and discriminate between the variants (Supplementary Table 4).

Amplification - SSIV One-Step RT-PCR System

The SuperScript™ IV One-Step RT-PCR System (Invitrogen, ThermoFisher Scientific) was used to amplify nucleic acid according to the manufacturer's instructions, using custom primer pools in 25 µL reactions. Primer pools were made at 10 µM. The following thermal cycling conditions were used: (1) reverse-transcription incubation at 50 °C for 15 min; (2) enzyme activation at 98 °C for 2 min (3) 35-40 cycles of 98 °C for 10 s, 60 °C for 10 s, and 72 °C for 1 min 30 s; (4) final extension at 72 °C for 5 min. Amplified samples were directly added into the detection reaction or stored at −20 °C until use.

Detection

We followed the methods under „General mCARMEN Procedures - Detection" with the following modifications: 42.5 nM LwaCas13 and 2-212.5 nM crRNA in each assay mix reaction.

Data analysis

Threshold calculation:

To determine if an ancestral or derived sequence is present, the signals between respective ancestral and mutation crRNA pairs must be evaluated and compared (Supplementary Table 4). First, background subtracted reporter fluorescence is normalized to the background subtracted passive reference dye (ROX) fluorescence for each assay in the IFC. Next, the ancestral:mutation and mutation:ancestral ratios are calculated for each five minute-interval time point across 180 minutes. For each crRNA pair, the ratio reaching a crRNA pair-specific threshold at the earliest time point is selected. If the ancestral:mutation ratio is selected, then the sequence present is determined to be ancestral. If the mutation:ancestral ratio is selected,

then the sequence present is determined to contain the mutation targeted by the mutation crRNA within the SARS-CoV-2 spike gene. crRNA pair-specific thresholds were determined based on ancestral and variant control samples, also referred to as the seedstock samples, tested in parallel with the unknown samples. For a given crRNA pair, the threshold was set to the lowest value with the maximum combined sensitivity and specificity when applied to the seedstock samples. For crRNA‟s detecting a SNP at the same position, the second lowest threshold with the maximum combined sensitivity and specificity was chosen if possible without compromising the maximum combined sensitivity and specificity. For crRNA pairs targeting mutations not represented in the variant control samples, a default crRNA pair threshold of 1.5 was set.

“Variant Identified” hit calling parameters:

1) If no mutations are detected, a result of “Ancestral” is returned.
2) At least one unique crRNA specific to a single SARS-CoV-2 variant must be above the fluorescence ratio threshold. If there is not one unique crRNA signal above threshold, a result of “Variant Not Identified” will be returned.
3) If two or more mutations for a given variant fall below the threshold, a result of “Variant Not Identified” will be returned. All other mutations must surpass the threshold.
4) If three or more unexpected mutations for a given variant are above threshold, a result of “Variant Not Identified” will be returned. At most, two unexpected signals can occur as long as parameters 1 and 2 are met.

If all three parameters are met, the result of “Variant Identified” will be returned. If the parameters are not met, a result of “Variant Not Identified” will be returned. Samples that contain additional mutation signals that fall outside of the typical variant lineage mutation list follow the below parameters. If 1-2 unexpected signals are observed slightly above threshold yet all other signals are correct for a specific variant lineage then the unexpected signal will be disregarded and the variant call will be made on the remaining signals. If more than two unexpected signals are observed above threshold and either all other signals are correct for a specific variant lineage or are not perfectly matching a result of “Variant Uncertain” will be returned.

*We would like to note that the variant identification pipeline will need to be updated as new SARS-CoV-2 mutations and variant lineages arise for proper identification.

There are a few exceptions worth mentioning: we observed crRNAs for SNPs E484Q, P681R, N501T, and L452Q, had undesirable cross-reactive signals with a position matched or adjacent mutation, and were, thus, excluded from further evaluation.

Citations

1. Mina, M. J. & Andersen, K. G. COVID-19 testing: One size does not fit all. *Science* vol. 371 126–127 (2021).
2. Rasmussen, A. L. & Popescu, S. V. SARS-CoV-2 transmission without symptoms. *Science* **371**, 1206–1207 (2021).
3. Winichakoon, P. *et al.* Negative Nasopharyngeal and Oropharyngeal Swabs Do Not Rule Out COVID-19. *J. Clin. Microbiol.* **58**, (2020).
4. Woloshin, S., Patel, N. & Kesselheim, A. S. False Negative Tests for SARS-CoV-2 Infection - Challenges and Implications. *N. Engl. J. Med.* **383**, e38 (2020).
5. Lemieux, J. E. *et al.* Phylogenetic analysis of SARS-CoV-2 in Boston highlights the impact of superspreading events. *Science* **371**, (2021).
6. Harvey, W. T. *et al.* SARS-CoV-2 variants, spike mutations and immune escape. *Nature Reviews Microbiology* vol. 19 409–424 (2021).
7. Dyson, L. *et al.* Possible future waves of SARS-CoV-2 infection generated by variants of concern with a range of characteristics. *Nat. Commun.* **12**, 1–13 (2021).
8. Zou, L. *et al.* SARS-CoV-2 Viral Load in Upper Respiratory Specimens of Infected Patients. *N. Engl. J. Med.* **382**, 1177–1179 (2020).
9. Wölfel, R. *et al.* Virological assessment of hospitalized patients with COVID-2019. *Nature* **581**, 465–469 (2020).
10. Vogels, C. B. F. *et al.* Multiplex qPCR discriminates variants of concern to enhance global surveillance of SARS-CoV-2. *PLoS Biol.* **19**, e3001236 (2021).
11. Heggestad, J. T. *et al.* Multiplexed, quantitative serological profiling of COVID-19 from blood by a point-of-care test. *Sci Adv* **7**, (2021).

12. Pham, J. *et al.* Performance Characteristics of a High-Throughput Automated Transcription-Mediated Amplification Test for SARS-CoV-2 Detection. *J. Clin. Microbiol.* **58**, (2020).
13. Eckbo, E. J. *et al.* Evaluation of the BioFire® COVID-19 test and Respiratory Panel 2.1 for rapid identification of SARS-CoV-2 in nasopharyngeal swab samples. *Diagn. Microbiol. Infect. Dis.* **99**, 115260 (2021).
14. Konings, F. *et al.* SARS-CoV-2 Variants of Interest and Concern naming scheme conducive for global discourse. *Nat Microbiol* **6**, 821–823 (2021).
15. Huang, H.-S. *et al.* Multiplex PCR system for the rapid diagnosis of respiratory virus infection: systematic review and meta-analysis. *Clin. Microbiol. Infect.* **24**, 1055–1063 (2018).
16. Jacky, L. *et al.* Robust Multichannel Encoding for Highly Multiplexed Quantitative PCR. *Anal. Chem.* **93**, 4208–4216 (2021).
17. Burki, T. Understanding variants of SARS-CoV-2. *Lancet* **397**, 462 (2021).
18. Borges, V. *et al.* Tracking SARS-CoV-2 lineage B.1.1.7 dissemination: insights from nationwide spike gene target failure (SGTF) and spike gene late detection (SGTL) data, Portugal, week 49 2020 to week 3 2021. *Euro Surveill.* **26**, (2021).
19. Xuan, J., Yu, Y., Qing, T., Guo, L. & Shi, L. Next-generation sequencing in the clinic: promises and challenges. *Cancer Lett.* **340**, 284–295 (2013).
20. Houldcroft, C. J., Beale, M. A. & Breuer, J. Clinical and biological insights from viral genome sequencing. *Nat. Rev. Microbiol.* **15**, 183–192 (2017).
21. Peddu, V. *et al.* Metagenomic Analysis Reveals Clinical SARS-CoV-2 Infection and Bacterial or Viral Superinfection and Colonization. *Clin. Chem.* **66**, 966–972 (2020).
22. Brito, A. F. *et al.* Global disparities in SARS-CoV-2 genomic surveillance. *medRxiv* (2021) doi:10.1101/2021.08.21.21262393.
23. Kaminski, M. M., Abudayyeh, O. O., Gootenberg, J. S., Zhang, F. & Collins, J. J. CRISPR-based diagnostics. *Nature Biomedical Engineering* **5**, 643–656 (2021).

24. Jiao, C. *et al.* Noncanonical crRNAs derived from host transcripts enable multiplexable RNA detection by Cas9. *Science* **372**, 941–948 (2021).
25. Gootenberg, J. S. *et al.* Multiplexed and portable nucleic acid detection platform with Cas13, Cas12a, and Csm6. *Science* **360**, 439–444 (2018).
26. Chen, J. S. *et al.* CRISPR-Cas12a target binding unleashes indiscriminate single-stranded DNase activity. *Science* **360**, 436–439 (2018).
27. Li, S.-Y. *et al.* CRISPR-Cas12a-assisted nucleic acid detection. *Cell Discov* **4**, 20 (2018).
28. Abudayyeh, O. O. *et al.* C2c2 is a single-component programmable RNA-guided RNA-targeting CRISPR effector. *Science* **353**, aaf5573 (2016).
29. Gootenberg, J. S. *et al.* Nucleic acid detection with CRISPR-Cas13a/C2c2. *Science* **356**, 438–442 (2017).
30. Myhrvold, C. *et al.* Field-deployable viral diagnostics using CRISPR-Cas13. *Science* **360**, 444–448 (2018).
31. Arizti-Sanz, J. *et al.* Streamlined inactivation, amplification, and Cas13-based detection of SARS-CoV-2. *Nat. Commun.* **11**, 5921 (2020).
32. Broughton, J. P. *et al.* CRISPR-Cas12-based detection of SARS-CoV-2. *Nat. Biotechnol.* **38**, (2020).
33. Patchsung, M. *et al.* Clinical validation of a Cas13-based assay for the detection of SARS-CoV-2 RNA. *Nature biomedical engineering* **4**, (2020).
34. Liu, T. Y. *et al.* Accelerated RNA detection using tandem CRISPR nucleases. *Nat. Chem. Biol.* **17**, (2021).
35. Metsky, H. C. *et al.* Designing sensitive viral diagnostics with machine learning. *Nat. Biotech.* doi:10.1038/s41587-022-01213-5 (2022).
36. Joung, J. *et al.* Detection of SARS-CoV-2 with SHERLOCK One-Pot Testing. *N. Engl. J. Med.* **383**, 1492–1494 (2020).
37. Bruch, R., Urban, G. A. & Dincer, C. CRISPR/Cas Powered Multiplexed Biosensing. *Trends*

Biotechnol. **37**, 791–792 (2019).

38. Tian *et al.* Exploiting the orthogonal CRISPR-Cas12a/Cas13a trans-cleavage for dual-gene virus detection using a handheld device. *Biosensors and Bioelectronics* vol. 196 113701 (2022).
39. Bruch, R. *et al.* CRISPR-powered electrochemical microfluidic multiplexed biosensor for target amplification-free miRNA diagnostics. *Biosensors and Bioelectronics* vol. 177 112887 (2021).
40. Ackerman, C. M. *et al.* Massively multiplexed nucleic acid detection with Cas13. *Nature* **582**, 277–282 (2020).
41. Crowe, J. E. Human Respiratory Viruses☆. *Reference Module in Biomedical Sciences* (2014) doi:10.1016/b978-0-12-801238-3.02600-3.
42. García Fernández, X., Álvarez-Argüelles, M. E., Rojo, S. & de-Oña, M. Stability of viral RNA in clinical specimens for viral diagnosis. *Enferm. Infecc. Microbiol. Clin.* **38**, 297–298 (2020).
43. Palmenberg, A. C. *et al.* Sequencing and analyses of all known human rhinovirus genomes reveal structure and evolution. *Science* **324**, 55–59 (2009).
44. Mackay, I. M., Arden, K. E. & Nitsche, A. Real-time PCR in virology. *Nucleic Acids Res.* **30**, 1292–1305 (2002).
45. Pulliam, J. R. C. *et al.* Increased risk of SARS-CoV-2 reinfection associated with emergence of the Omicron variant in South Africa. *medRxiv* 2021.11.11.21266068 (2021).
46. Brandal, L. T. *et al.* Outbreak caused by the SARS-CoV-2 Omicron variant in Norway, November to December 2021. *Euro Surveill.* **26**, (2021).
47. CDC COVID-19 Response Team. SARS-CoV-2 B.1.1.529 (Omicron) Variant - United States, December 1-8, 2021. *MMWR Morb. Mortal. Wkly. Rep.* **70**, 1731–1734 (2021).
48. Li, A., Maier, A., Carter, M. & Guan, T. H. Omicron and S-gene target failure cases in the

highest COVID-19 case rate region in Canada-December 2021. *J. Med. Virol.* (2021) doi:10.1002/jmv.27562.

49. Kirkland, P. D. & Frost, M. J. The impact of viral transport media on PCR assay results for the detection of nucleic acid from SARS-CoV-2. *Pathology* **52**, 811–814 (2020).
50. Fozouni, P. *et al.* Amplification-free detection of SARS-CoV-2 with CRISPR-Cas13a and mobile phone microscopy. *Cell* **184**, 323–333.e9 (2021).
51. Nalefski, E. A. *et al.* Kinetic analysis of Cas12a and Cas13a RNA-Guided nucleases for development of improved CRISPR-Based diagnostics. *iScience* **24**, 102996 (2021).
52. Thakku, S. G. *et al.* Multiplexed detection of bacterial nucleic acids using Cas13 in droplet microarrays. *bioRxiv* 2021.11.12.468388 (2021) doi:10.1101/2021.11.12.468388.
53. Barnes, K. G. *et al.* Deployable CRISPR-Cas13a diagnostic tools to detect and report Ebola and Lassa virus cases in real-time. *Nat. Commun.* **11**, 4131 (2020).
54. Katoh, K. & Standley, D. M. MAFFT Multiple Sequence Alignment Software Version 7: Improvements in Performance and Usability. *Mol. Biol. Evol.* **30**, 772–780 (2013).
55. Matranga, C. B. *et al.* Enhanced methods for unbiased deep sequencing of Lassa and Ebola RNA viruses from clinical and biological samples. *Genome Biol.* **15**, 519 (2014).

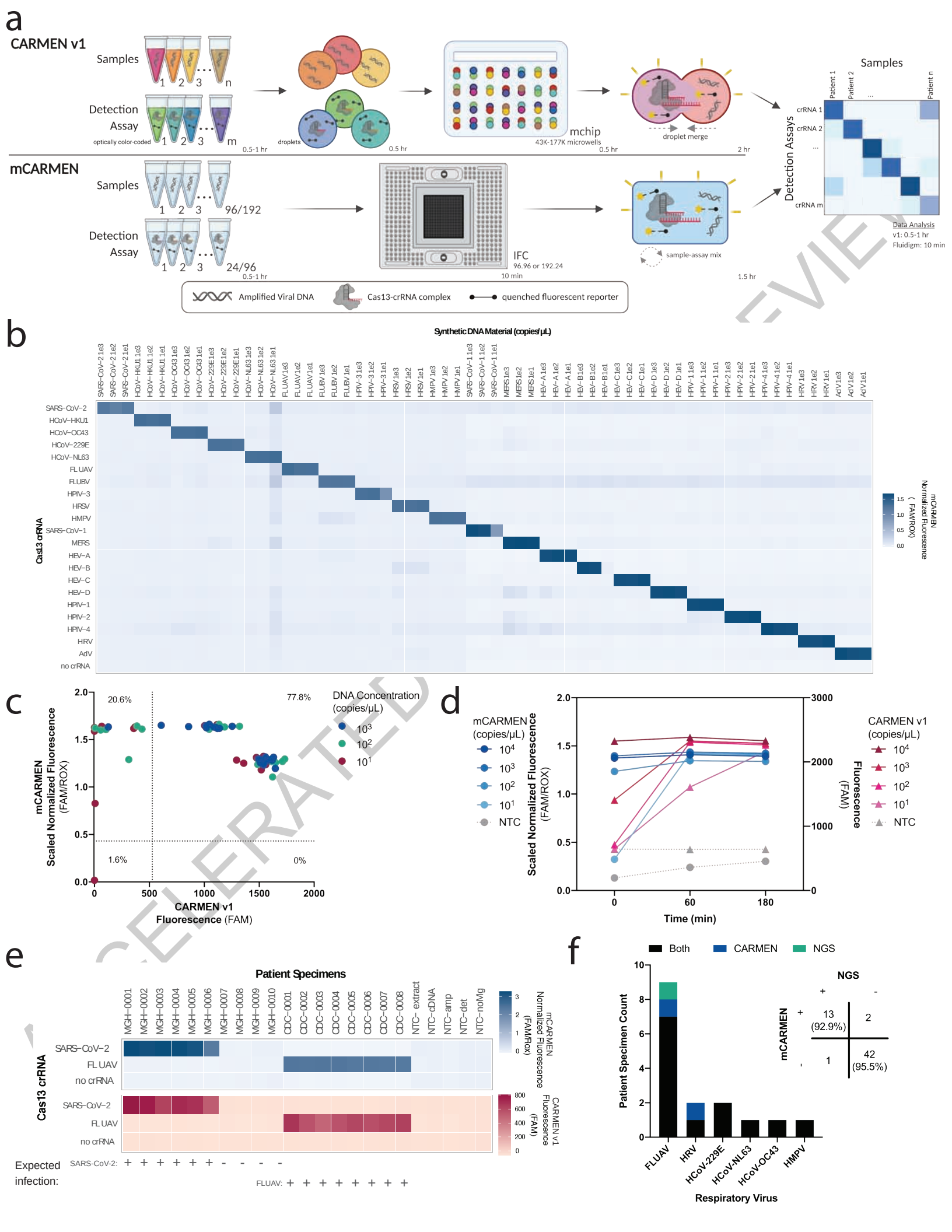

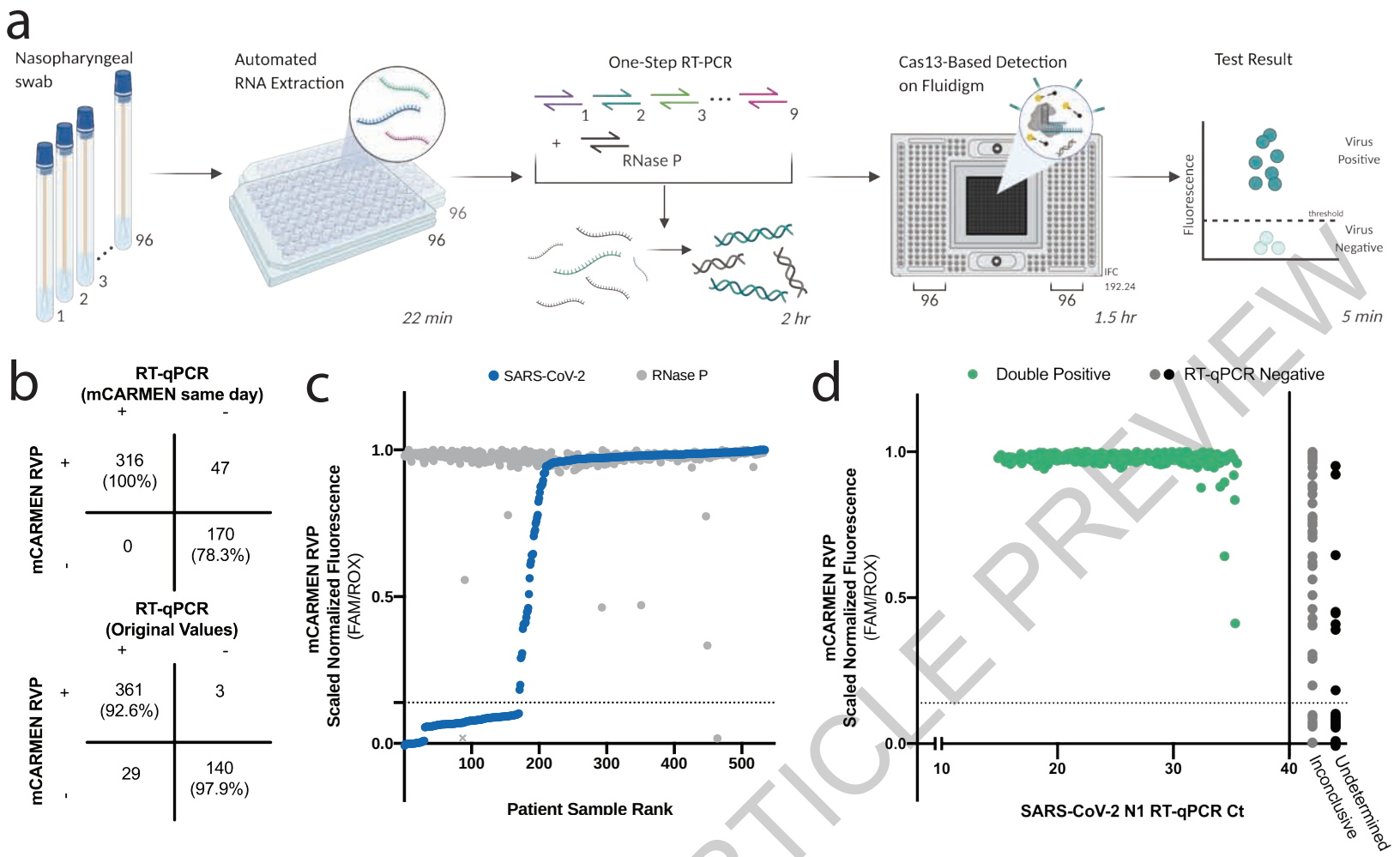

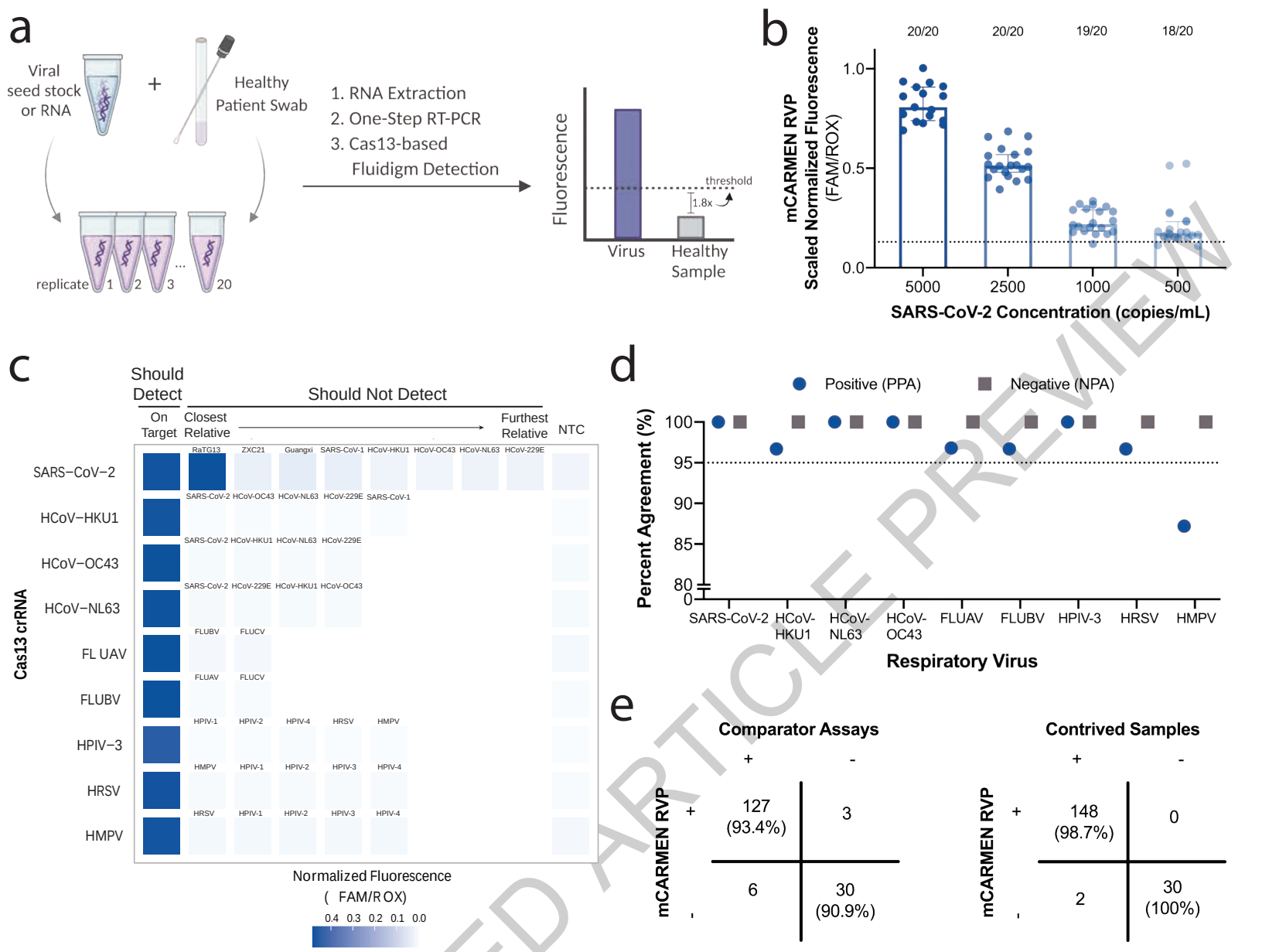

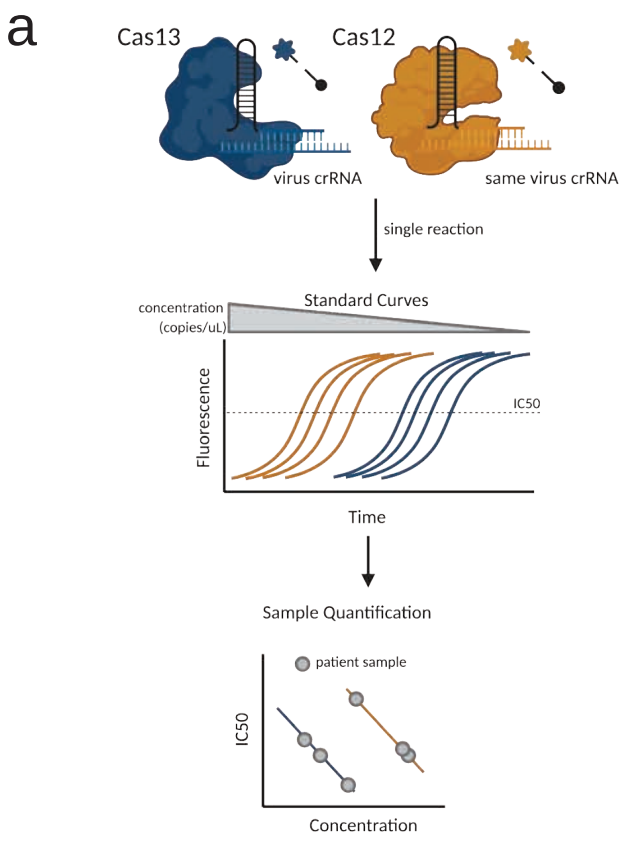

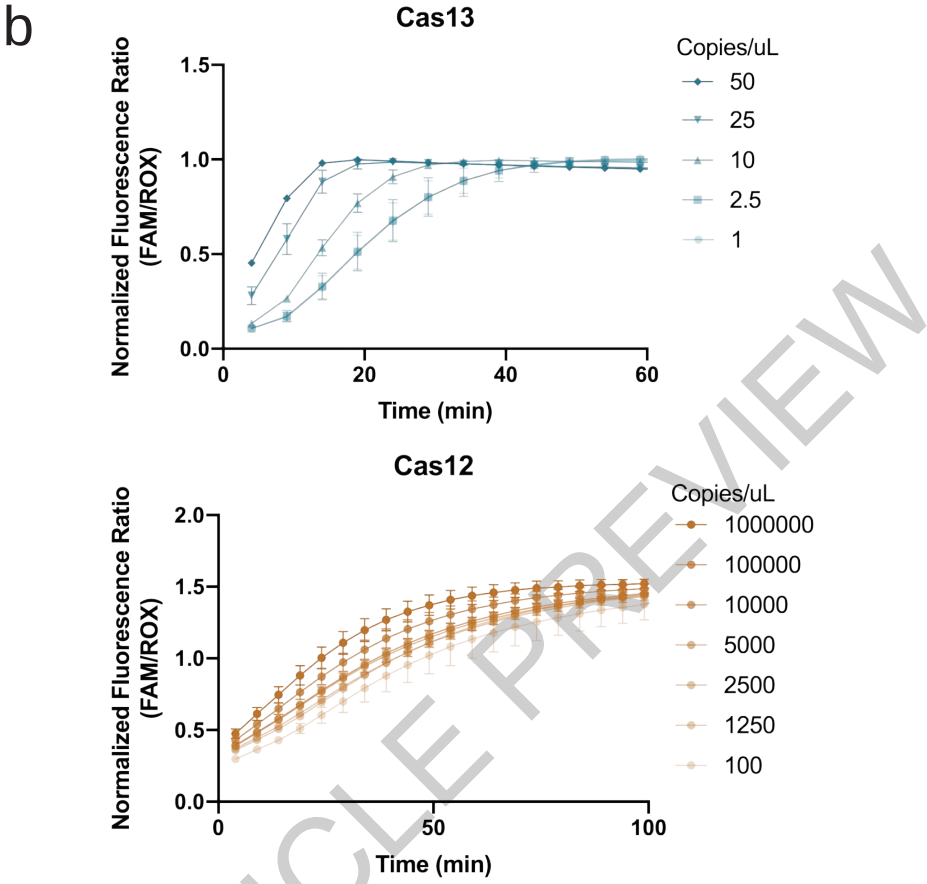

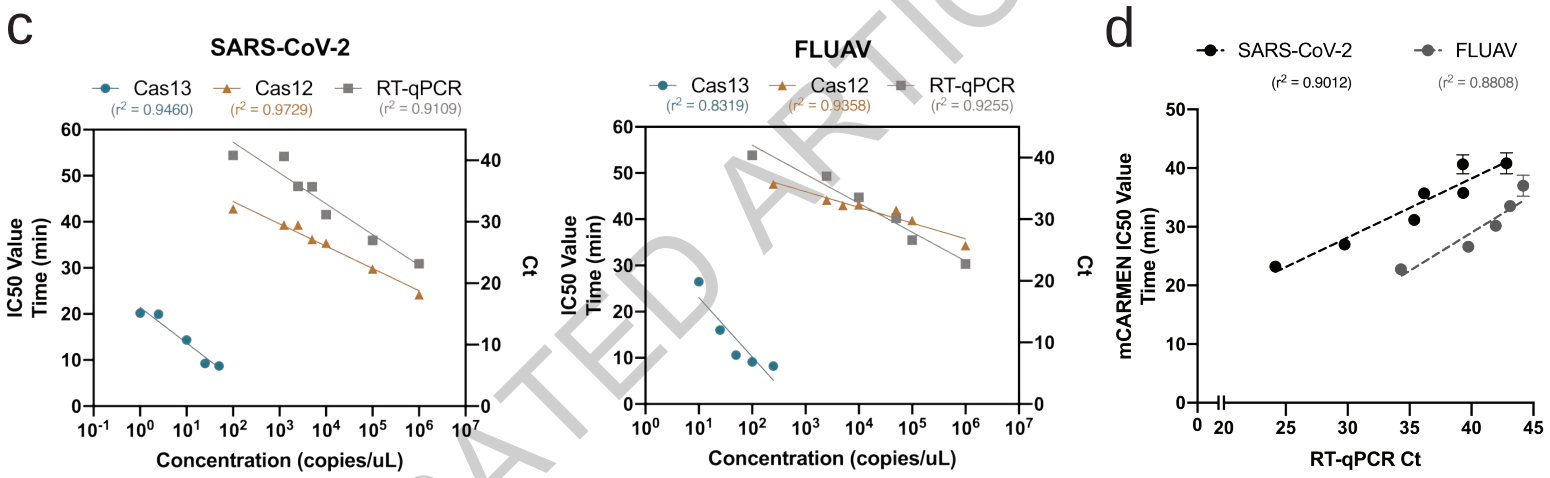

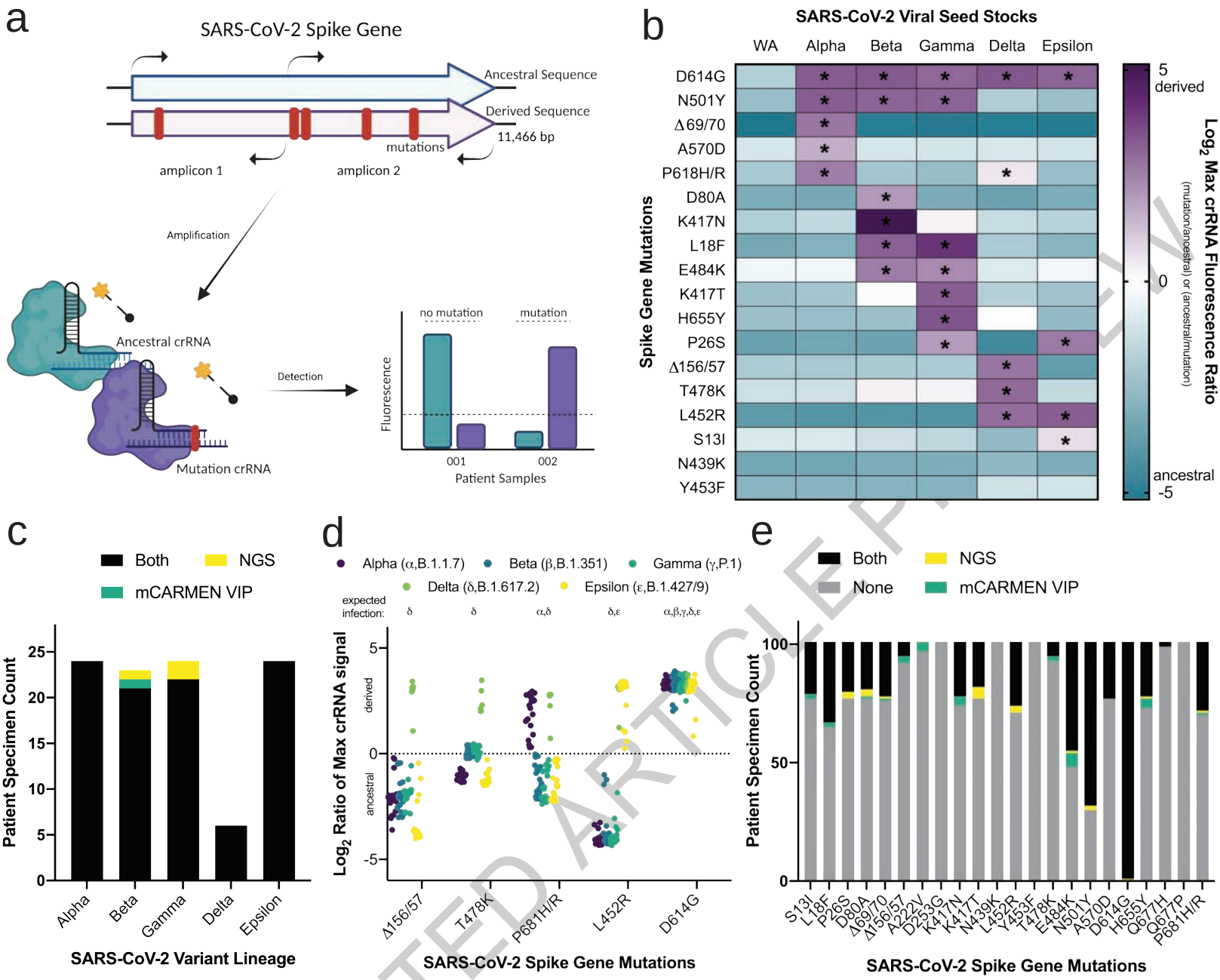

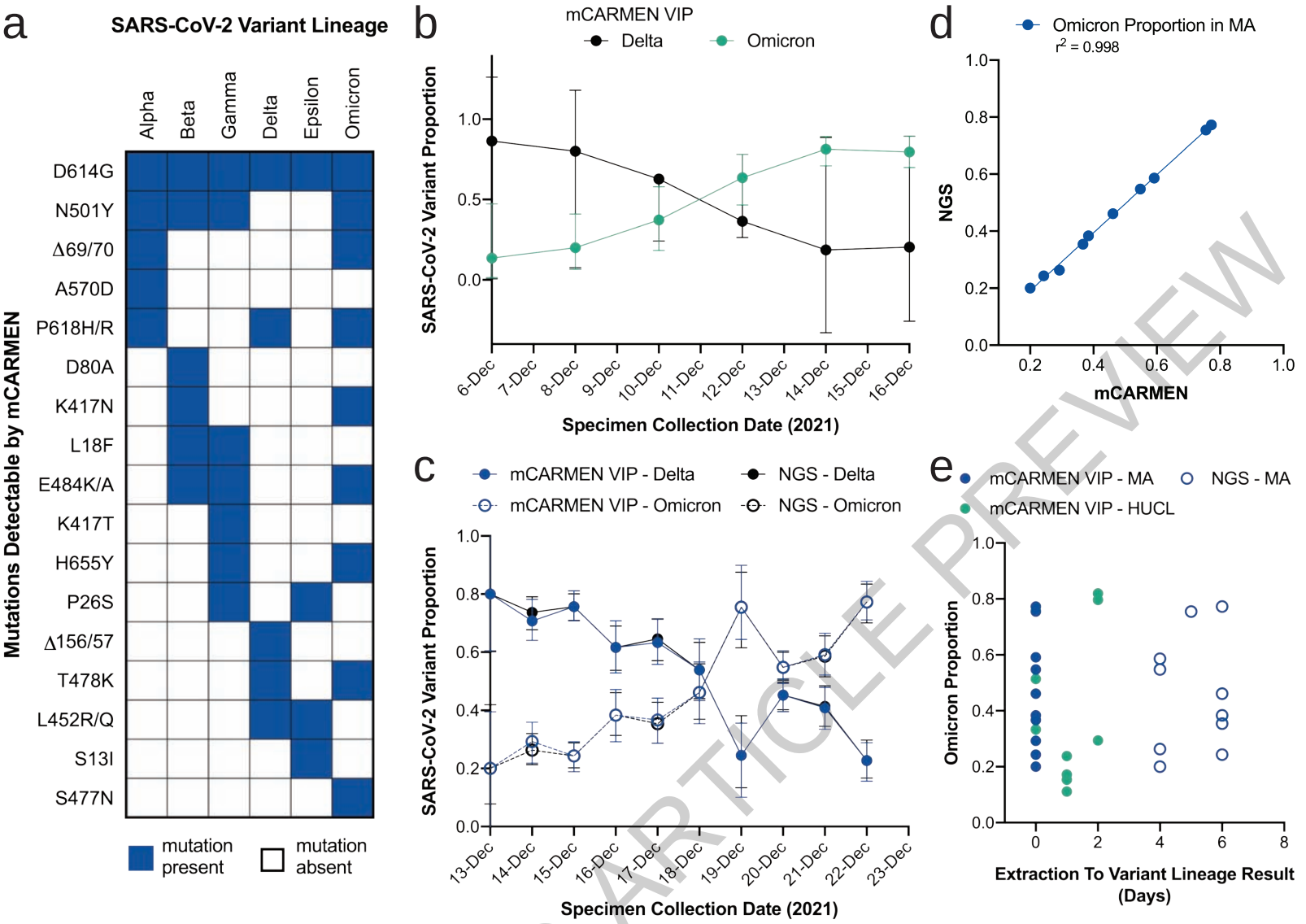

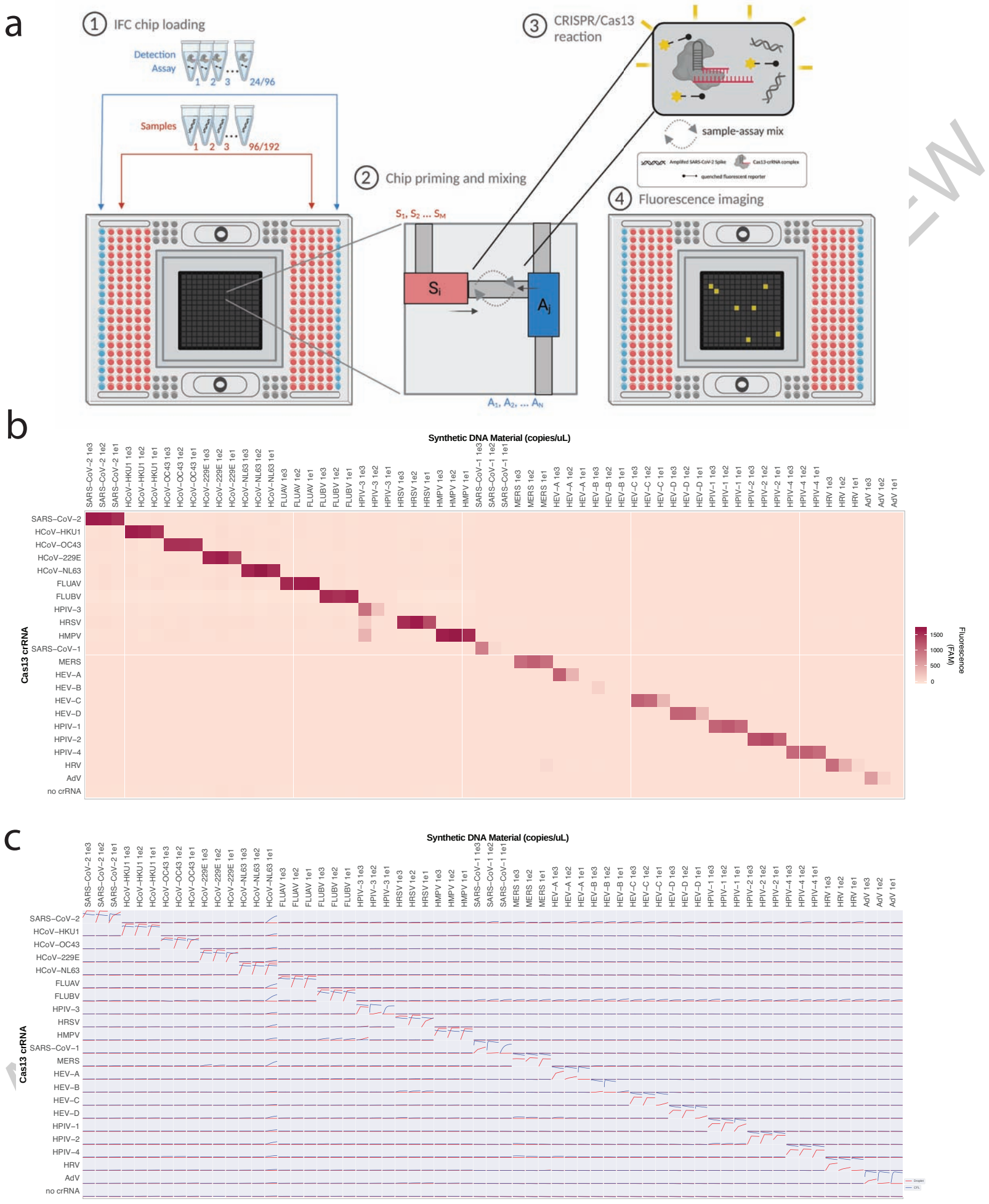
a
1 IFC chip loading
Detection Assay
1 2 3 24/96
Samples
1 2 3 96/192
2 Chip priming and mixing
S1, S2 ... SM
Si
Aj
A1, A2, ... AN
3 CRISPR/Cas13 reaction
sample-assay mix
Amplified SARS-CoV-2 Spike
Cas13-crRNA complex
quenched fluorescent reporter
4 Fluorescence imaging
b
Synthetic DNA Material (copies/uL)
SARS–CoV–2 1e3
SARS–CoV–2 1e2
SARS–CoV–2 1e1
HCoV–HKU1 1e3
HCoV–HKU1 1e2
HCoV–HKU1 1e1
HCoV–OC43 1e3
HCoV–OC43 1e2
HCoV–OC43 1e1
HCoV–229E 1e3
HCoV–229E 1e2
HCoV–229E 1e1
HCoV–NL63 1e3
HCoV–NL63 1e2
HCoV–NL63 1e1
FLUAV 1e3
FLUAV 1e2
FLUAV 1e1
FLUBV 1e3
FLUBV 1e2
FLUBV 1e1
HPIV–3 1e3
HPIV–3 1e2
HPIV–3 1e1
HRSV 1e3
HRSV 1e2
HRSV 1e1
HMPV 1e3
HMPV 1e2
HMPV 1e1
SARS–CoV–1 1e3
SARS–CoV–1 1e2
SARS–CoV–1 1e1
MERS 1e3
MERS 1e2
MERS 1e1
HEV–A 1e3
HEV–A 1e2
HEV–A 1e1
HEV–B 1e3
HEV–B 1e2
HEV–B 1e1
HEV–C 1e3
HEV–C 1e2
HEV–C 1e1
HEV–D 1e3
HEV–D 1e2
HEV–D 1e1
HPIV–1 1e3
HPIV–1 1e2
HPIV–1 1e1
HPIV–2 1e3
HPIV–2 1e2
HPIV–2 1e1
HPIV–4 1e3
HPIV–4 1e2
HPIV–4 1e1
HRV 1e3
HRV 1e2
HRV 1e1
AdV 1e3
AdV 1e2
AdV 1e1
Cas13 crRNA
SARS–CoV–2
HCoV–HKU1
HCoV–OC43
HCoV–229E
HCoV–NL63
FLUAV
FLUBV
HPIV–3
HRSV
HMPV
SARS–CoV–1
MERS
HEV–A
HEV–B
HEV–C
HEV–D
HPIV–1
HPIV–2
HPIV–4
HRV
AdV
no crRNA
1500
1000
500
0
Fluorescence (FAM)
c
Synthetic DNA Material (copies/uL)
Cas13 crRNA

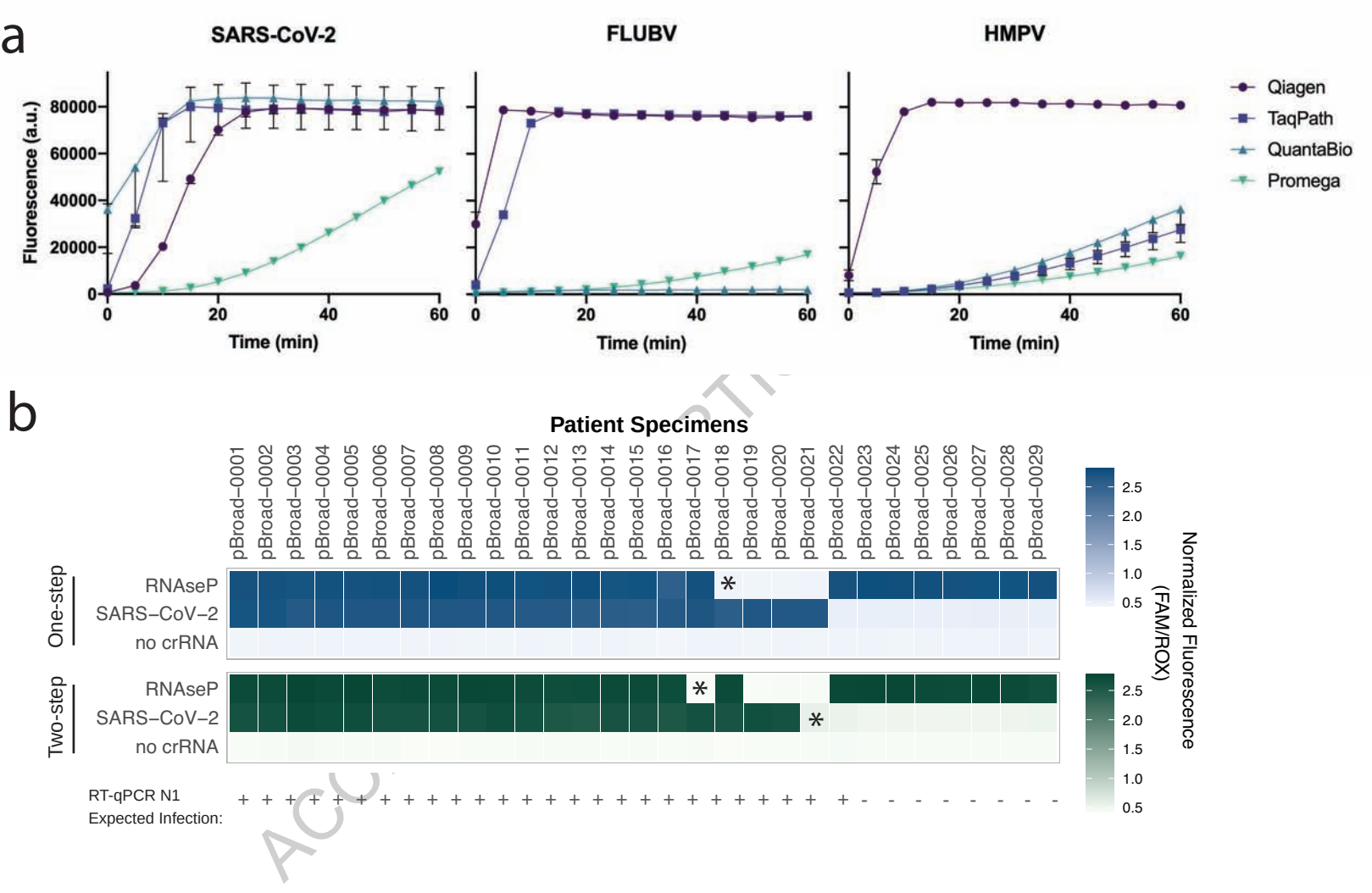
a
SARS-CoV-2
FLUBV
HMPV
Fluorescence (a.u.)
80000
60000
40000
20000
0
0
20
40
60
Time (min)
Qiagen
TaqPath
QuantaBio
Promega
b
Patient Specimens
pBroad–0001
pBroad–0002
pBroad–0003
pBroad–0004
pBroad–0005
pBroad–0006
pBroad–0007
pBroad–0008
pBroad–0009
pBroad–0010
pBroad–0011
pBroad–0012
pBroad–0013
pBroad–0014
pBroad–0015
pBroad–0016
pBroad–0017
pBroad–0018
pBroad–0019
pBroad–0020
pBroad–0021
pBroad–0022
pBroad–0023
pBroad–0024
pBroad–0025
pBroad–0026
pBroad–0027
pBroad–0028
pBroad–0029
One-step
RNAseP
SARS–CoV–2
no crRNA
Two-step
RNAseP
SARS–CoV–2
no crRNA
RT-qPCR N1
Expected Infection:
Normalized Fluorescence (FAM/ROX)
2.5
2.0
1.5
1.0
0.5

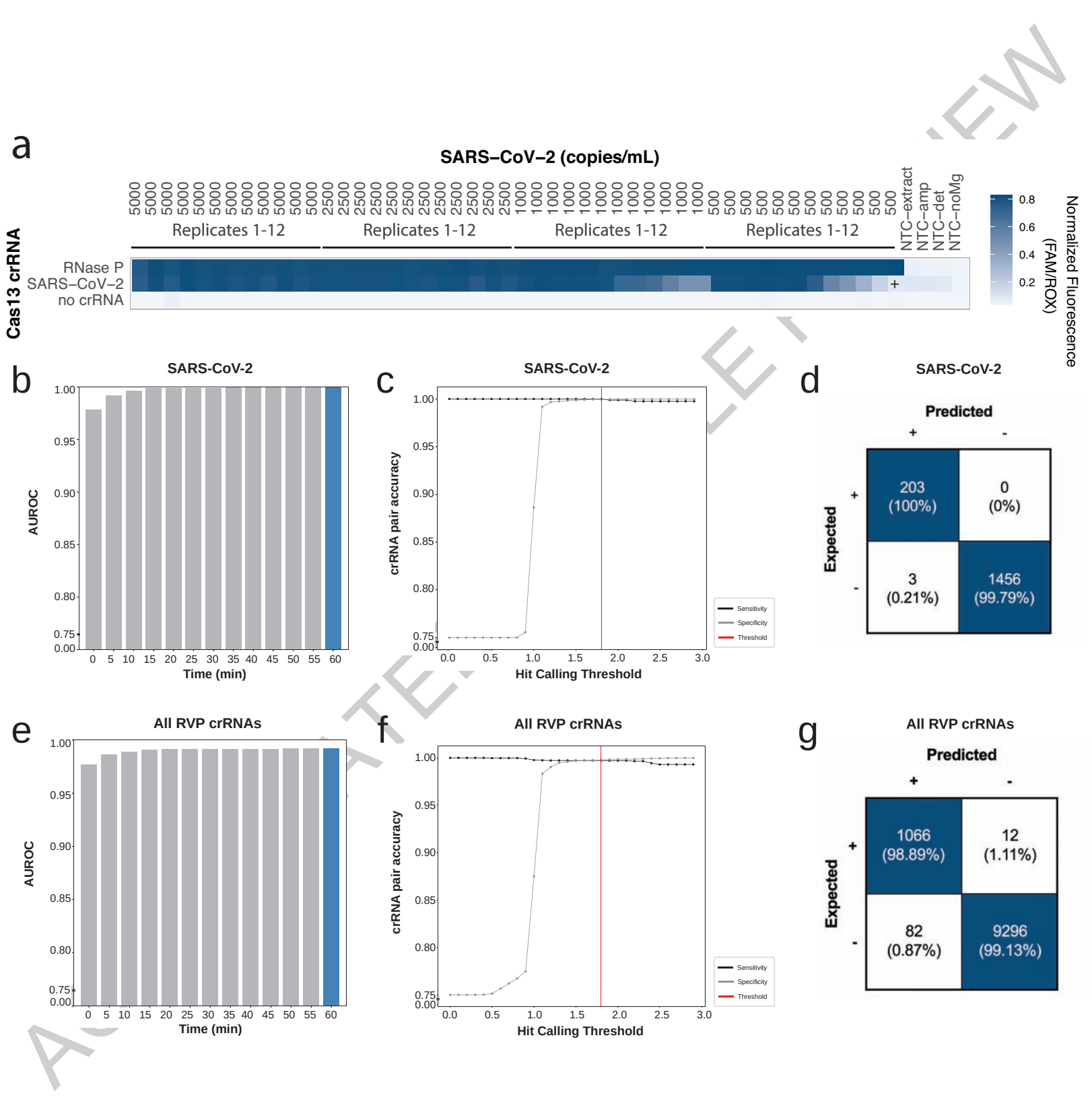
a
SARS–CoV–2 (copies/mL)
5000 5000 5000 5000 5000 5000 5000 5000 5000 5000 5000 5000
2500 2500 2500 2500 2500 2500 2500 2500 2500 2500 2500 2500
1000 1000 1000 1000 1000 1000 1000 1000 1000 1000 1000 1000
500 500 500 500 500 500 500 500 500 500 500 500
Replicates 1-12
Replicates 1-12
Replicates 1-12
Replicates 1-12
NTC–extract
NTC–amp
NTC–det
NTC–noMg
Cas13 crRNA
RNase P
SARS–CoV–2
no crRNA
+
Normalized Fluorescence (FAM/ROX)
0.8
0.6
0.4
0.2
b
SARS-CoV-2
AUROC
Time (min)
c
SARS-CoV-2
crRNA pair accuracy
Hit Calling Threshold
Sensitivity
Specificity
Threshold
d
SARS-CoV-2
Predicted
Expected
203 (100%)
0 (0%)
3 (0.21%)
1456 (99.79%)
e
All RVP crRNAs
AUROC
Time (min)
f
All RVP crRNAs
crRNA pair accuracy
Hit Calling Threshold
Sensitivity
Specificity
Threshold
g
All RVP crRNAs
Predicted
Expected
1066 (98.89%)
12 (1.11%)
82 (0.87%)
9296 (99.13%)

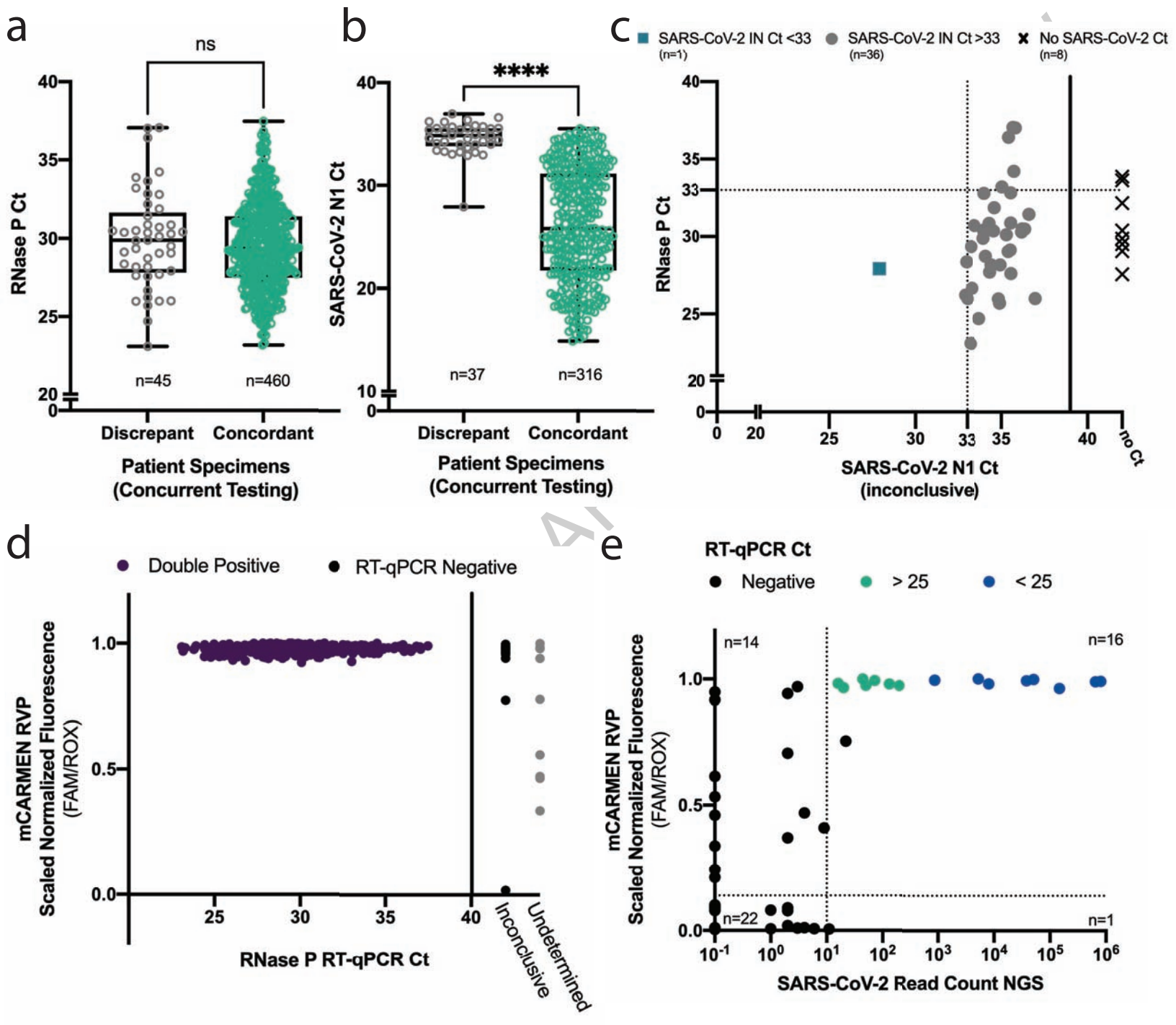
a
ns
RNase P Ct
n=45
n=460
Discrepant
Concordant
Patient Specimens
(Concurrent Testing)
b
****
SARS-CoV-2 N1 Ct
n=37
n=316
Discrepant
Concordant
Patient Specimens
(Concurrent Testing)
c
SARS-CoV-2 IN Ct <33
(n=1)
SARS-CoV-2 IN Ct >33
(n=36)
No SARS-CoV-2 Ct
(n=8)
RNase P Ct
SARS-CoV-2 N1 Ct
(inconclusive)
no Ct
d
Double Positive
RT-qPCR Negative
mCARMEN RVP
Scaled Normalized Fluorescence
(FAM/ROX)
RNase P RT-qPCR Ct
Inconclusive
Undetermined
e
RT-qPCR Ct
Negative
> 25
< 25
n=14
n=16
n=22
n=1
mCARMEN RVP
Scaled Normalized Fluorescence
(FAM/ROX)
SARS-CoV-2 Read Count NGS

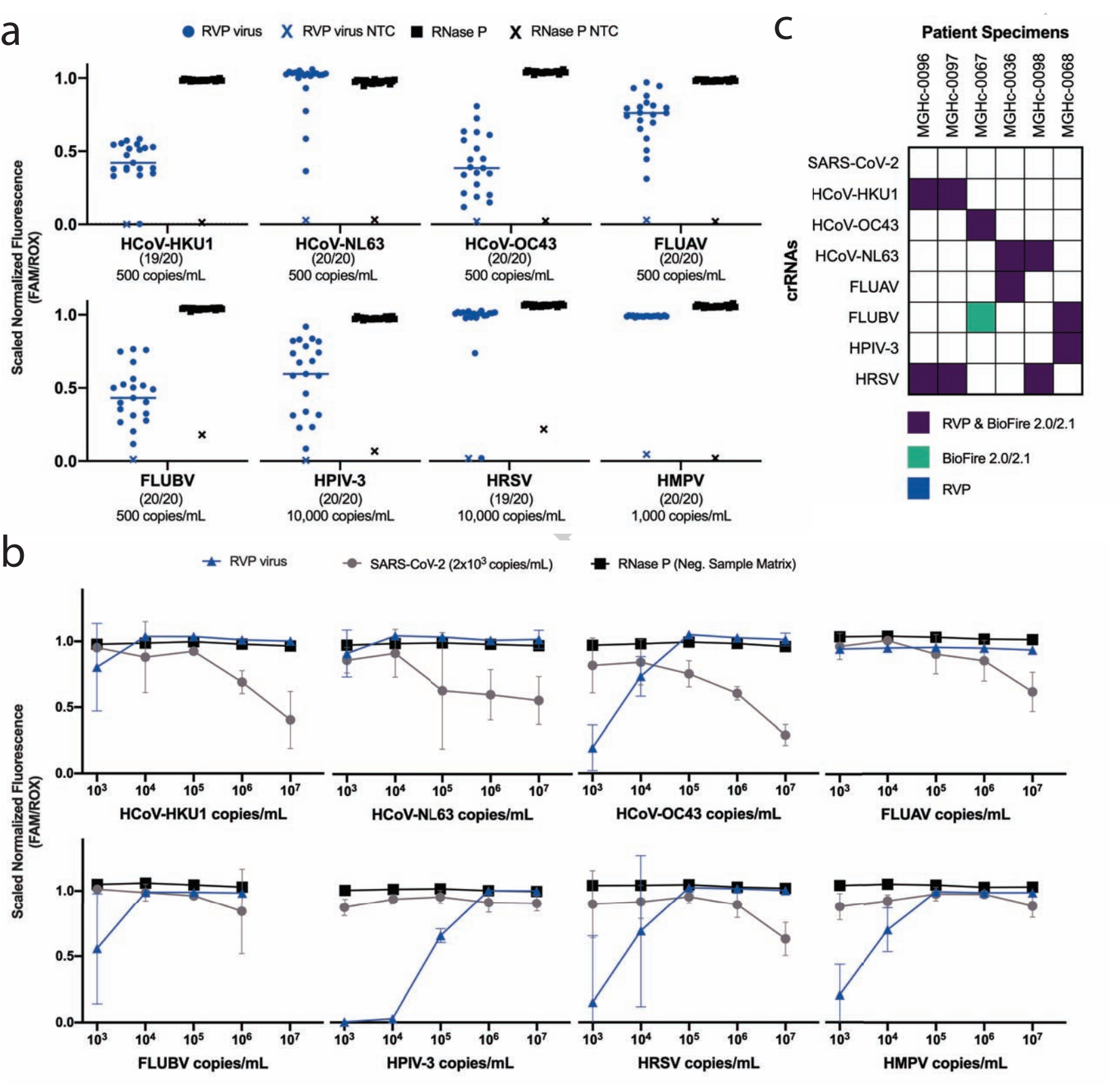
a
RVP virus
RVP virus NTC
RNase P
RNase P NTC
Scaled Normalized Fluorescence (FAM/ROX)
HCoV-HKU1 (19/20) 500 copies/mL
HCoV-NL63 (20/20) 500 copies/mL
HCoV-OC43 (20/20) 500 copies/mL
FLUAV (20/20) 500 copies/mL
FLUBV (20/20) 500 copies/mL
HPIV-3 (20/20) 10,000 copies/mL
HRSV (19/20) 10,000 copies/mL
HMPV (20/20) 1,000 copies/mL
c
Patient Specimens
MGHc-0096
MGHc-0097
MGHc-0067
MGHc-0036
MGHc-0098
MGHc-0068
crRNAs
SARS-CoV-2
HCoV-HKU1
HCoV-OC43
HCoV-NL63
FLUAV
FLUBV
HPIV-3
HRSV
RVP & BioFire 2.0/2.1
BioFire 2.0/2.1
RVP
b
RVP virus
SARS-CoV-2 (2x10³ copies/mL)
RNase P (Neg. Sample Matrix)
Scaled Normalized Fluorescence (FAM/ROX)
HCoV-HKU1 copies/mL
HCoV-NL63 copies/mL
HCoV-OC43 copies/mL
FLUAV copies/mL
FLUBV copies/mL
HPIV-3 copies/mL
HRSV copies/mL
HMPV copies/mL

a

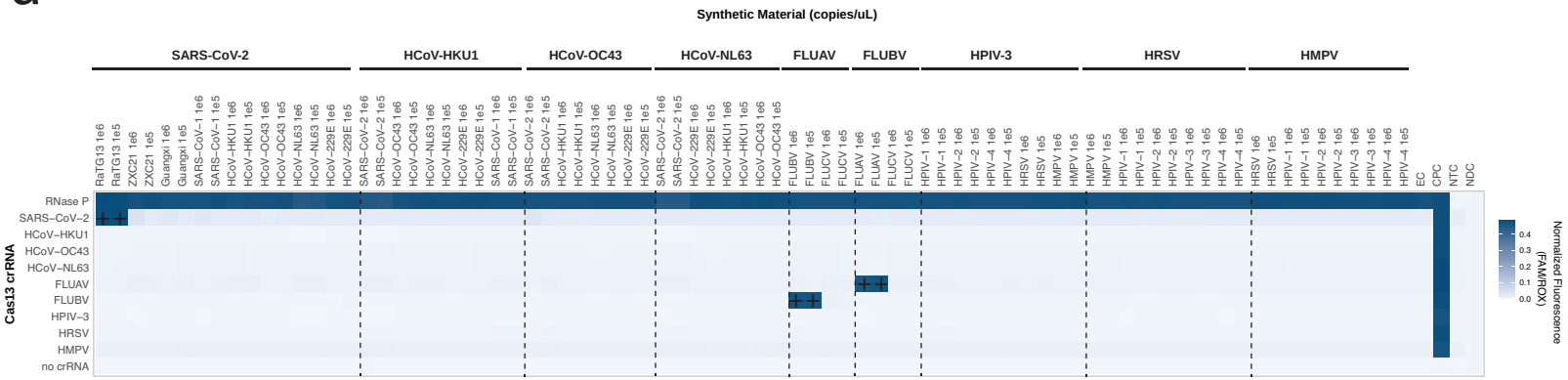

b

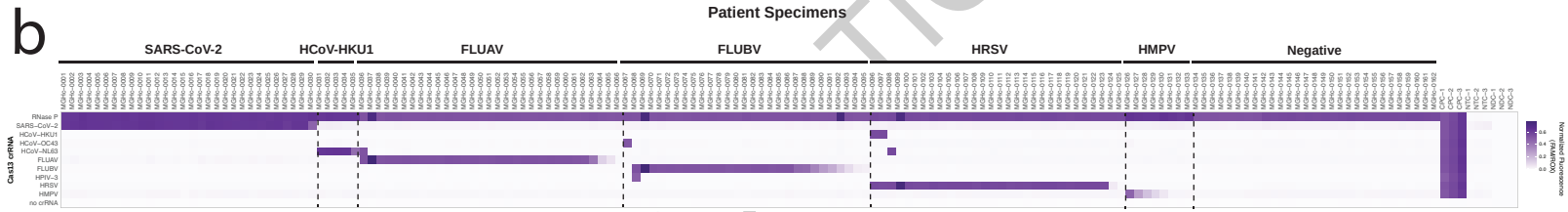

c

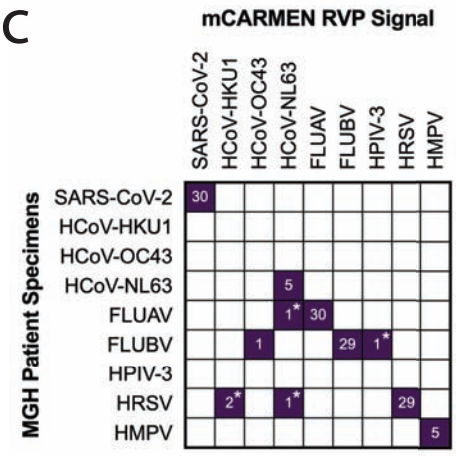

a

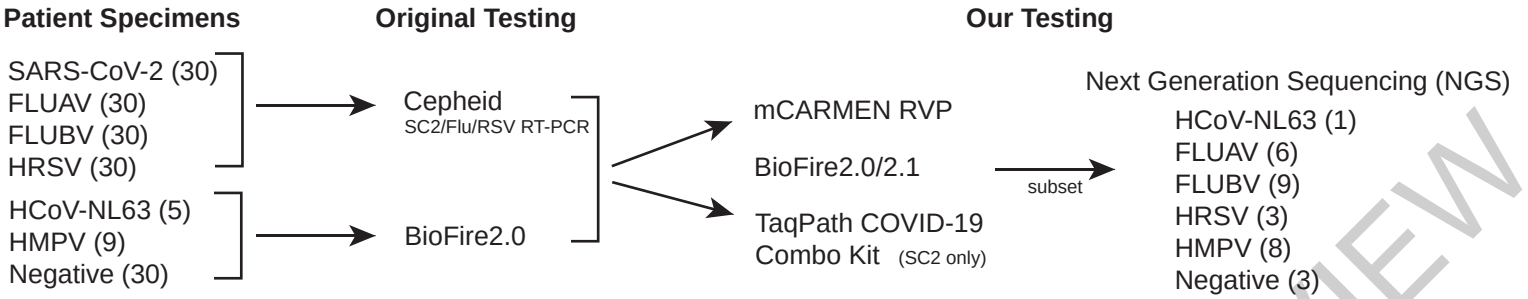
Patient Specimens
Original Testing
Our Testing
SARS-CoV-2 (30)
FLUAV (30)
FLUBV (30)
HRSV (30)
HCoV-NL63 (5)
HMPV (9)
Negative (30)
Cepheid
SC2/Flu/RSV RT-PCR
BioFire2.0
mCARMEN RVP
BioFire2.0/2.1
TaqPath COVID-19
Combo Kit (SC2 only)
subset
Next Generation Sequencing (NGS)
HCoV-NL63 (1)
FLUAV (6)
FLUBV (9)
HRSV (3)
HMPV (8)
Negative (3)

b

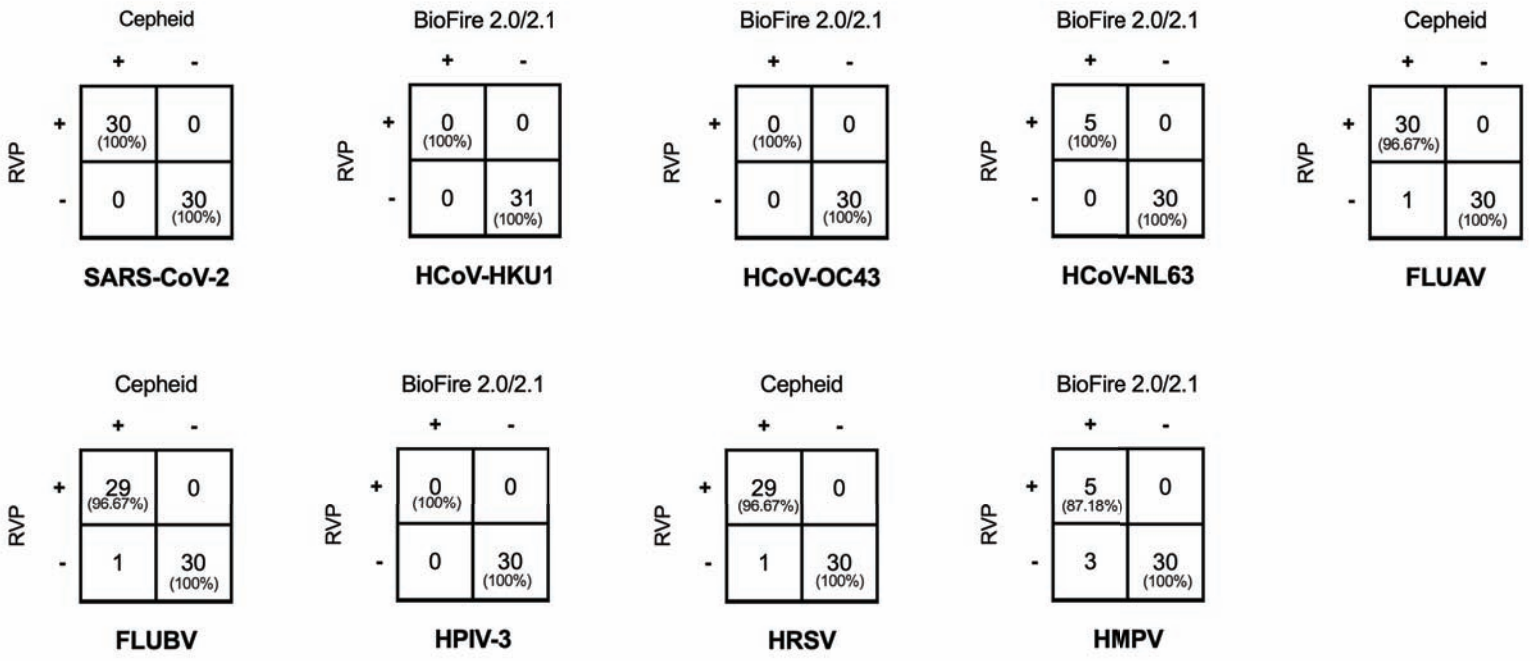
Cepheid
RVP
30 (100%)
0
0
30 (100%)
SARS-CoV-2
BioFire 2.0/2.1
0 (100%)
0
0
31 (100%)
HCoV-HKU1
BioFire 2.0/2.1
0 (100%)
0
0
30 (100%)
HCoV-OC43
BioFire 2.0/2.1
5 (100%)
0
0
30 (100%)
HCoV-NL63
Cepheid
30 (96.67%)
0
1
30 (100%)
FLUAV
Cepheid
29 (96.67%)
0
1
30 (100%)
FLUBV
BioFire 2.0/2.1
0 (100%)
0
0
30 (100%)
HPIV-3
Cepheid
29 (96.67%)
0
1
30 (100%)
HRSV
BioFire 2.0/2.1
5 (87.18%)
0
3
30 (100%)
HMPV

c

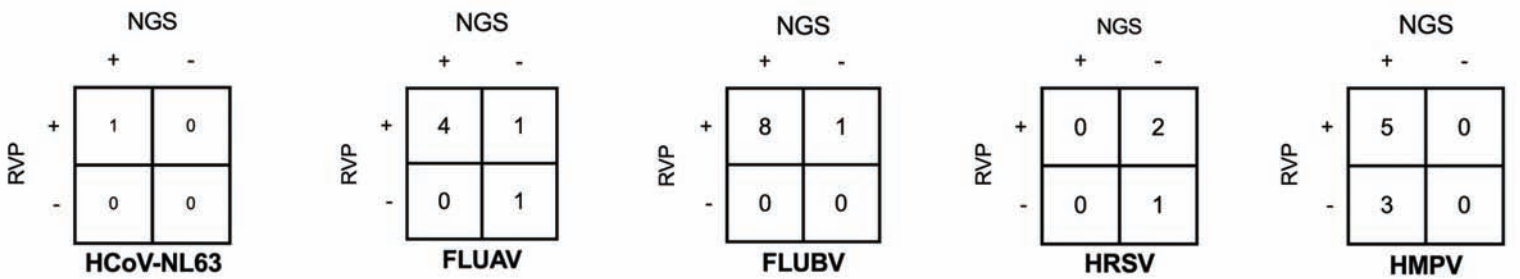
NGS
RVP
1
0
0
0
HCoV-NL63
NGS
4
1
0
1
FLUAV
NGS
8
1
0
0
FLUBV
NGS
0
2
0
1
HRSV
NGS
5
0
3
0
HMPV

d

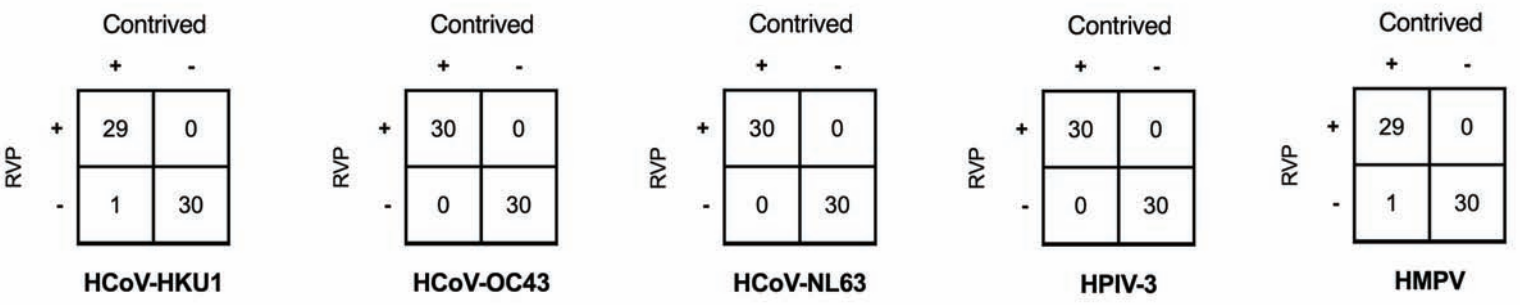
Contrived
RVP
29
0
1
30
HCoV-HKU1
Contrived
30
0
0
30
HCoV-OC43
Contrived
30
0
0
30
HCoV-NL63
Contrived
30
0
0
30
HPIV-3
Contrived
29
0
1
30
HMPV

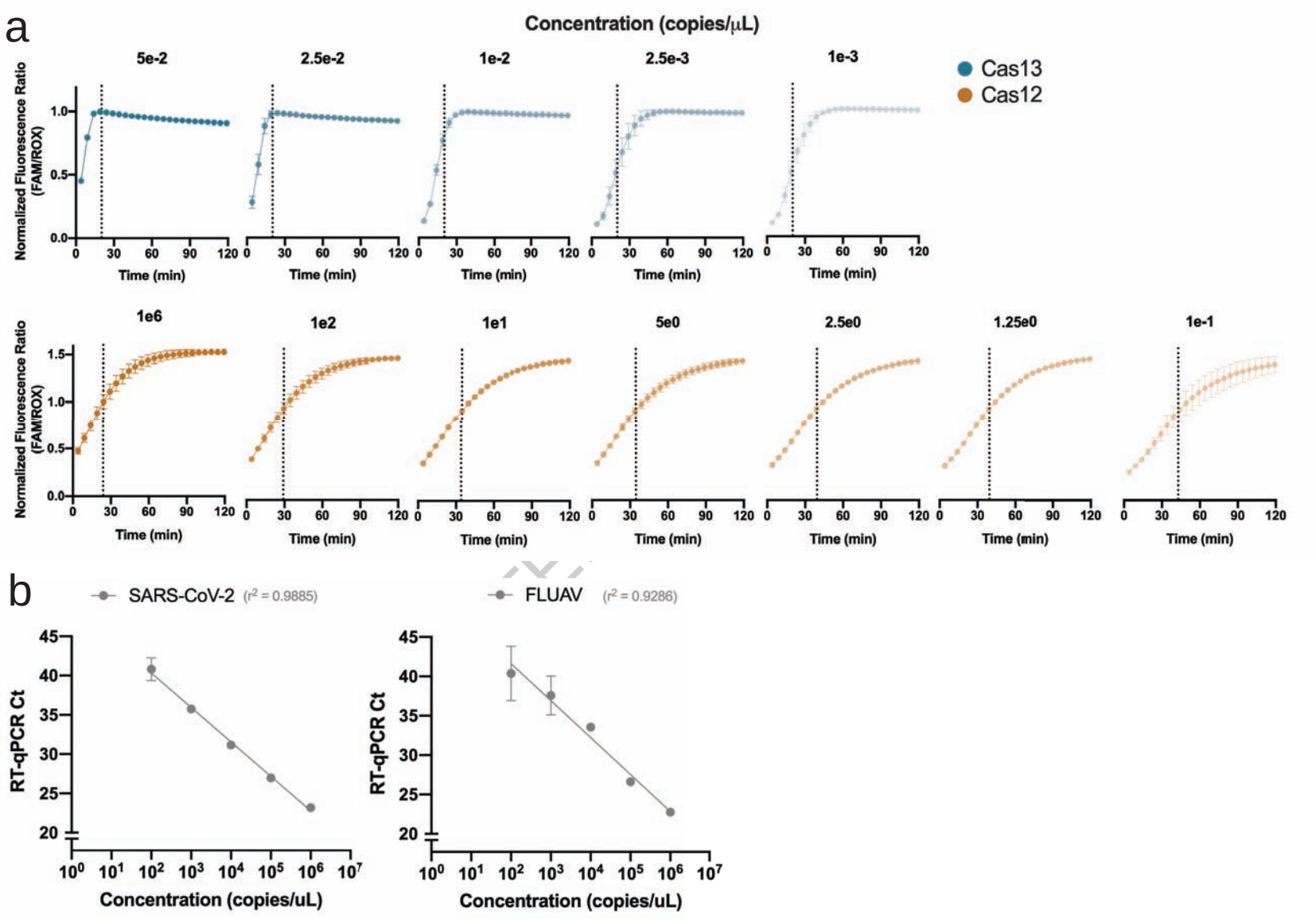
a
Concentration (copies/μL)
5e-2
2.5e-2
1e-2
2.5e-3
1e-3
Cas13
Cas12
Normalized Fluorescence Ratio (FAM/ROX)
Time (min)
1e6
1e2
1e1
5e0
2.5e0
1.25e0
1e-1
b
SARS-CoV-2 (r² = 0.9885)
FLUAV (r² = 0.9286)
RT-qPCR Ct
Concentration (copies/uL)

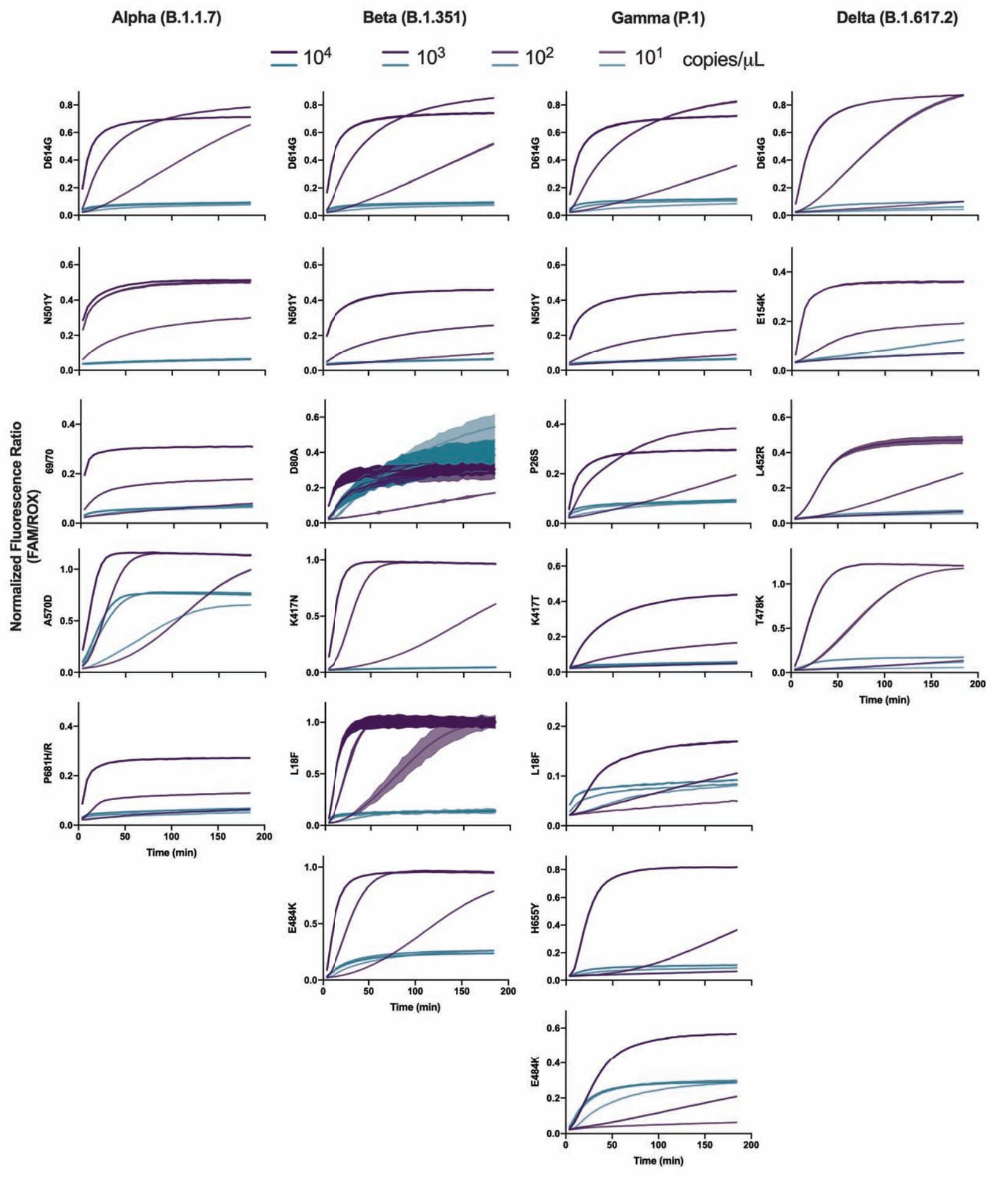
Alpha (B.1.1.7)
Beta (B.1.351)
Gamma (P.1)
Delta (B.1.617.2)
10^4
10^3
10^2
10^1 copies/µL
Normalized Fluorescence Ratio (FAM/ROX)
D614G
N501Y
69/70
A570D
P681H/R
D80A
K417N
L18F
E484K
P26S
K417T
H655Y
E154K
L452R
T478K
Time (min)

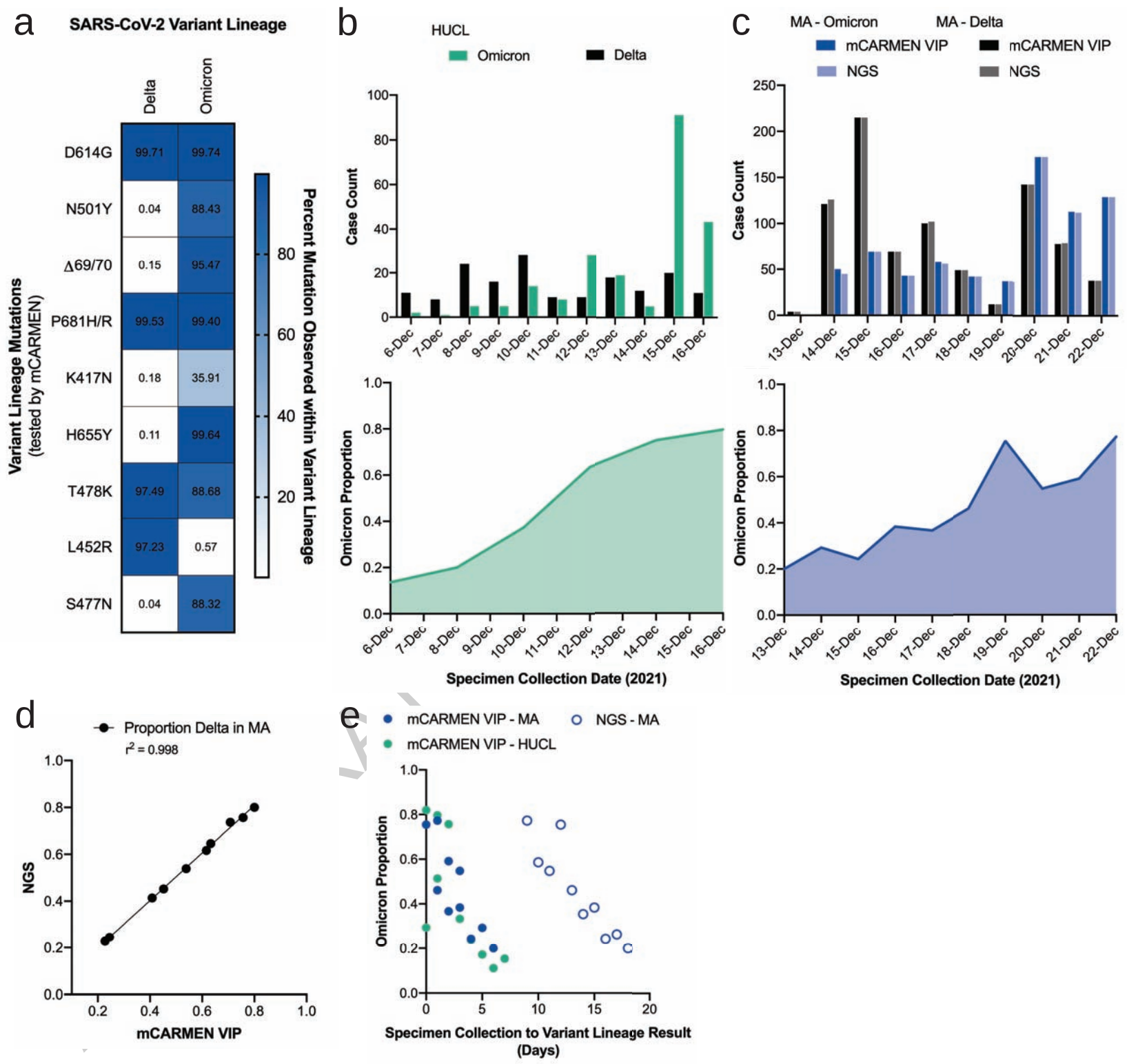
a
SARS-CoV-2 Variant Lineage
Delta
Omicron
D614G
N501Y
Δ69/70
P681H/R
K417N
H655Y
T478K
L452R
S477N
99.71
99.74
0.04
88.43
0.15
95.47
99.53
99.40
0.18
35.91
0.11
99.64
97.49
88.68
97.23
0.57
0.04
88.32
Variant Lineage Mutations
(tested by mCARMEN)
Percent Mutation Observed within Variant Lineage
80
60
40
20
b
HUCL
Omicron
Delta
Case Count
Omicron Proportion
6-Dec
7-Dec
8-Dec
9-Dec
10-Dec
11-Dec
12-Dec
13-Dec
14-Dec
15-Dec
16-Dec
Specimen Collection Date (2021)
c
MA - Omicron
MA - Delta
mCARMEN VIP
NGS
Case Count
Omicron Proportion
13-Dec
14-Dec
15-Dec
16-Dec
17-Dec
18-Dec
19-Dec
20-Dec
21-Dec
22-Dec
Specimen Collection Date (2021)
d
Proportion Delta in MA
r² = 0.998
NGS
mCARMEN VIP
e
mCARMEN VIP - MA
NGS - MA
mCARMEN VIP - HUCL
Omicron Proportion
Specimen Collection to Variant Lineage Result
(Days)

nature portfolio

Corresponding author(s): Nicole Welch, Cameron Myhrvold, Pardis Sabeti

Last updated by author(s): Feb 1, 2022

Reporting Summary

Nature Portfolio wishes to improve the reproducibility of the work that we publish. This form provides structure for consistency and transparency in reporting. For further information on Nature Portfolio policies, see our Editorial Policies and the Editorial Policy Checklist.

Statistics

For all statistical analyses, confirm that the following items are present in the figure legend, table legend, main text, or Methods section.

n/a	Confirmed
☐	☒ The exact sample size (*n*) for each experimental group/condition, given as a discrete number and unit of measurement
☐	☒ A statement on whether measurements were taken from distinct samples or whether the same sample was measured repeatedly
☐	☒ The statistical test(s) used AND whether they are one- or two-sided *Only common tests should be described solely by name; describe more complex techniques in the Methods section.*
☐	☒ A description of all covariates tested
☐	☒ A description of any assumptions or corrections, such as tests of normality and adjustment for multiple comparisons
☐	☒ A full description of the statistical parameters including central tendency (e.g. means) or other basic estimates (e.g. regression coefficient) AND variation (e.g. standard deviation) or associated estimates of uncertainty (e.g. confidence intervals)
☐	☒ For null hypothesis testing, the test statistic (e.g. *F*, *t*, *r*) with confidence intervals, effect sizes, degrees of freedom and *P* value noted *Give P values as exact values whenever suitable.*
☒	☐ For Bayesian analysis, information on the choice of priors and Markov chain Monte Carlo settings
☒	☐ For hierarchical and complex designs, identification of the appropriate level for tests and full reporting of outcomes
☒	☐ Estimates of effect sizes (e.g. Cohen's *d*, Pearson's *r*), indicating how they were calculated

Our web collection on statistics for biologists contains articles on many of the points above.

Software and code

Policy information about availability of computer code

Data collection	Data was collected on the Fluidigm Biomark. Droplet data was collected using Matlab 2013 for microscope and camera control.
Data analysis	Python3 custom analysis codes available on github: broadinstitute/mcarmen, MAFFT v7 and ADAPT were used for primer design, crRNA design and in silico specificity analysis. RStudio 4 and Prism 9 were used for plotting.

For manuscripts utilizing custom algorithms or software that are central to the research but not yet described in published literature, software must be made available to editors and reviewers. We strongly encourage code deposition in a community repository (e.g. GitHub). See the Nature Portfolio guidelines for submitting code & software for further information.

Data

Policy information about availability of data

All manuscripts must include a data availability statement. This statement should provide the following information, where applicable:

- Accession codes, unique identifiers, or web links for publicly available datasets
- A description of any restrictions on data availability
- For clinical datasets or third party data, please ensure that the statement adheres to our policy

Sequencing data will be made publicly available on the SRA under the BioProject Accession # PRJNA802370. Raw data may be made available upon request.

Field-specific reporting

Please select the one below that is the best fit for your research. If you are not sure, read the appropriate sections before making your selection.

☒ Life sciences ☐ Behavioural & social sciences ☐ Ecological, evolutionary & environmental sciences

For a reference copy of the document with all sections, see nature.com/documents/nr-reporting-summary-flat.pdf

Life sciences study design

All studies must disclose on these points even when the disclosure is negative.

Sample size	No sample-size calculations were performed. Samples evaluated were based on availability or FDA standards for clinical validation.
Data exclusions	There were only two samples that were excluded from data analysis. One SARS-CoV-2 positive sample tested in an academic setting that was positive by RT-qPCR but by mCARMEN signal was was too high in every crRNA channel including negative controls and thus had to be excluded because proper call could not be made. One HCoV-HKU1 sample from clinical evaluation at MGH was excluded because it tested positive for HCoV-HKU1 by BioFire, but upon repeated tested by BioFire, mCARMEN, and NGS there was no human internal control detected and there were minimal human reads suggesting the sample was heavily degraded. Since initial submission more samples have been excluded. There were 8 samples excluded from Fig. 2 because they did not pass quality control metrics set by the CDC nCoV-2019 ROU kit for RNase P. There were also samples excluded from Fig. 6 that did not contain enough viral RNA resulting in a Variant Not Identified (VNI) call by our analysis pipeline. All samples tested where known positive by RT-qPCR however leftover material was given for our evaluation resulting in not enough material in several cases thus the samples were excluded.
Replication	Each experiment includes at least 2 technical replicates per data point and up to 20 replicates for limit of detection experiments. Patient sample testing was done over multiple experiments and days. All attempts at data replication were successful.
Randomization	Samples were not randomized into groups, as samples were not grouped.
Blinding	Blinding was performed for the 58 presumed respiratory virus sample testing. Blinding was not possible for some samples due to the nature of the patient cohorts selected (they were known to be disease-positive).

Reporting for specific materials, systems and methods

We require information from authors about some types of materials, experimental systems and methods used in many studies. Here, indicate whether each material, system or method listed is relevant to your study. If you are not sure if a list item applies to your research, read the appropriate section before selecting a response.

Materials & experimental systems

n/a	Involved in the study
☒	☐ Antibodies
☒	☐ Eukaryotic cell lines
☒	☐ Palaeontology and archaeology
☒	☐ Animals and other organisms
☐	☒ Human research participants
☒	☐ Clinical data
☒	☐ Dual use research of concern

Methods

n/a	Involved in the study
☒	☐ ChIP-seq
☒	☐ Flow cytometry
☒	☐ MRI-based neuroimaging

Human research participants

Policy information about studies involving human research participants

Population characteristics	Population characteristics are unknown for all specimens in this study. Specimens were collected throughout the state of Massachusetts specifically at Broad Institute's Genomics Platform CLIA Laboratory, Massachusetts General Hospital, and Harvard Longwood Campus, but were provided de-identified for our use in this manuscript.
Recruitment	No recruitment was done for this study. Specimens were provided by the Broad Institute's Genomics Platform CLIA Laboratory, Massachusetts General Hospital, and Harvard Longwood Campus.
Ethics oversight	Use of clinical excess of human specimens from patients with SARS-CoV-2 from the Broad Institute's Genomics Platform CLIA Laboratory was approved by the MIT IRB Protocol #1612793224. Additional SARS-CoV-2 samples were collected from consented individuals under Harvard Longwood Campus IRB #20-1877 and covered by an exempt determination (EX-7295) at the Broad Institute. Human specimens from patients with SARS-CoV-2, HCoV-HKU1, HCoV-NL63, FLUAV, FLUBV, HRSV, and HMPV were obtained under a waiver of consent from the Mass General Brigham IRB Protocol #2019P003305.

Note that full information on the approval of the study protocol must also be provided in the manuscript.